LIMNOLOGY and OCEANOGRAPHY

ASLO

Limnol. Oceanogr. 9999, 2020, 1–22

doi: 10.1002/lno.11405

Different carboxyl-rich alicyclic molecules proxy compounds select distinct bacterioplankton for oxidation of dissolved organic matter in the mesopelagic Sargasso Sea

Shuting Liu,[1*] **Rachel Parsons**,[2] **Keri Opalk**,[1] **Nicholas Baetge**,[1] **Stephen Giovannoni**,[3] **Luis M. Bolaños**,[3] **Elizabeth B. Kujawinski**,[4] **Krista Longnecker**,[4] **YueHan Lu**,[4,5] **Elisa Halewood**,[1] **Craig A. Carlson**[1]

[1]Marine Science Institute/Department of Ecology, Evolution and Marine Biology, University of California Santa Barbara, California
[2]Bermuda Institute of Ocean Sciences, St George's, Bermuda
[3]Department of Microbiology, Oregon State University, Corvallis, Oregon
[4]Department of Marine Chemistry and Geochemistry, Woods Hole Oceanographic Institution, Woods Hole, Massachusetts
[5]Department of Geological Sciences, University of Alabama, Tuscaloosa, Alabama

Abstract

Marine dissolved organic matter (DOM) varies in its recalcitrance to rapid microbial degradation. DOM of varying recalcitrance can be exported from the ocean surface to depth by subduction or convective mixing and oxidized over months to decades in deeper seawater. Carboxyl-rich alicyclic molecules (CRAM) are characterized as a major component of recalcitrant DOM throughout the oceanic water column. The oxidation of CRAM-like compounds may depend on specific bacterioplankton lineages with oxidative enzymes capable of catabolizing complex molecular structures like long-chain aliphatics, cyclic alkanes, and carboxylic acids. To investigate the interaction between bacteria and CRAM-like compounds, we conducted microbial remineralization experiments using several compounds rich in carboxyl groups and/or alicyclic rings, including deoxycholate, humic acid, lignin, and benzoic acid, as proxies for CRAM. Mesopelagic seawater (200 m) from the northwest Sargasso Sea was used as media and inoculum and incubated over 28 d. All amendments demonstrated significant DOC removal (2–11 μmol C L^{-1}) compared to controls. Bacterioplankton abundance increased significantly in the deoxycholate and benzoic acid treatments relative to controls, with fast-growing *Spongiibacteracea*, Euryarcheaota, and slow-growing SAR11 enriched in the deoxycholate treatment and fast-growing *Alteromonas*, Euryarcheaota, and Thaumarcheaota enriched in the benzoic acid treatment. In contrast, bacterioplankton grew slower in the lignin and humic acid treatments, with oligotrophic SAR202 becoming significantly enriched in the lignin treatment. Our results indicate that the character of the CRAM proxy compounds resulted in distinct bacterioplankton removal rates of DOM and affected specific lineages of bacterioplankton capable of responding.

Carboxyl-rich alicyclic molecules (CRAM), defined as a diverse array of organic compounds enriched with carboxylated and fused alicyclic rings, comprise some of the more recalcitrant compounds in the ocean (Hertkorn et al. 2006). Similar in structure to steroids and hopanoids, CRAM compounds are resistant to rapid microbial degradation (Hertkorn et al. 2006; Flerus et al. 2012; Lechtenfeld et al. 2014; Repeta 2015). While only ~3% of dissolved organic carbon (DOC) in the deep ocean can be characterized as specific biochemicals (Benner and Amon 2015), the broad group of CRAM compounds can account for ~8% of the bulk DOC in the open ocean, yet the dynamics of such compounds remain understudied.

DOC dynamics in the northwestern Sargasso Sea follow regular annual patterns of seasonal accumulation in the surface during summer, autumn stratified periods, and redistribution from the surface into the upper mesopelagic water during winter convective mixing (Carlson et al. 1994; Hansell and Carlson 2001). Convective mixing near the Bermuda Atlantic Time-series Study (BATS) site can extend deeper than 300 m, leading to DOC export of 0.3–1.4 mol m^{-2} y^{-1} from the

*Correspondence: shutingliu@ucsb.edu

Additional Supporting Information may be found in the online version of this article.

euphotic to the upper mesopelagic zone (100–300 m) (Carlson et al. 1994; Hansell and Carlson 2001). Exported DOC is of varying recalcitrance; some turns over on time scales of weeks to months (i.e., semi-labile DOC) and some turns over on time scales of years (i.e., semi-refractory DOC) (Hansell et al. 2012; Hansell 2013; Carlson and Hansell 2015).

During and shortly following deep convective mixing, bacterioplankton abundance increases within the upper mesopelagic zone at BATS (Carlson et al. 1996), coinciding with the timing of DOC removal within the upper mesopelagic (Carlson et al. 1994; Hansell and Carlson 2001). These dynamics suggest that a portion of the surface-accumulated DOC, which resists or escapes microbial degradation (including CRAM), is metabolized by mesopelagic bacterioplankton. This process may depend on specific bacterioplankton lineages with specialized metabolic pathways for catabolizing complex molecular structures, including long-chain aliphatics, cyclic alkanes, and carboxylic acids. For instance, single-amplified genomes from SAR202 subgroup III encode multiple families of oxidative enzymes involved in the degradation of cyclic alkanes. Landry et al. (2017) postulated that members of the SAR202 clade play an important role in oxidation of recalcitrant DOC. Previous studies at BATS have shown that SAR11 ecotypes Ib and II, marine *Actinobacteria*, SAR202, and OCS116 all increase in their relative abundance within the upper mesopelagic water during periods shortly following deep convective mixing (Morris et al. 2005; Carlson et al. 2009; Treusch et al. 2009), further suggesting that specific mesopelagic microbes are capable of responding to the flux of recalcitrant DOM compounds transported downward via convective mixing.

Studies have shown that DOC becomes diagenetically altered over time and depth through microbial processing. Goldberg et al. (2009) measured temporal changes of dissolved combined neutral sugars (DCNS) relative to DOC concentrations in the upper 300 m at BATS. Surface-accumulated DOC that was exported to the mesopelagic was degraded from spring to summer, resulting in a subsequent decrease in DCNS yield and change in the mole fraction of specific neutral sugars consistent with diagenetic alteration. Kaiser and Benner (2009) reported that carbon-normalized yields of amino acids, neutral sugars, and amino sugars decreased with depth at BATS, suggesting microbial transformation of DOC to more recalcitrant material over depth. Incubation studies have shown that measures of dissolved organic matter (DOM) composition, such as fluorescence from humic-like DOM, D-amino acid concentrations, and molecular features detected through Fourier-transform ion cyclotron resonance mass spectrometry (FTICR-MS), shift over long incubations (Kramer and Herndl 2004; Kawasaki and Benner 2006; Lonborg et al. 2009; Koch et al. 2014), indicating that microbial remineralization processes alter DOM quantity and quality.

The objective of this study was to examine the oxidation of CRAM-like compounds of varying recalcitrance by bacterioplankton in order to help predict the fate of exported DOM within the mesopelagic ocean. Results from mesopelagic bacterioplankton remineralization experiments indicate that specific bacterioplankton lineages were capable of remineralizing and transforming the various forms of amended CRAM proxies. These findings improve our understanding of linkages between lineage-specific bacterioplankton growth and DOM composition, thus, providing further insight into the strategies of carbon allocation and niche specialization in the oceanic water column.

Materials and methods

Experimental setup

Mesopelagic seawater (200 m) from Hydrostation S (32°10′N, 64°30′W) in the northwestern Sargasso Sea was collected onboard the R/V *Atlantic Explorer* via Niskin bottles on a conductivity, temperature, and depth (CTD) profiling rosette. Water was collected on 07 September 2016 when the water column was thermally stratified (mixed layer of 22 m). Concentrations of nitrate plus nitrite and phosphate were 1.30–1.44 μmol L^{-1} and 0.10–0.16 μmol L^{-1} at 200 m, respectively, not considered to be limiting to bacterioplankton (Carlson et al. 2004).

Natural assemblages of mesopelagic bacterioplankton were incubated in grazer-reduced seawater cultures and allowed to grow on naturally occurring substrates alone or in combination with organic amendments as described in Carlson et al. (2004). Briefly, seawater cultures were prepared by diluting whole (unfiltered) 200 m seawater by 70% with 0.2 μm mesopelagic filtrate (Carlson et al. 2004). The inoculum and filtrate were mixed within a 12 L polycarbonate carboy and then transferred to duplicate 5.5 L polycarbonate biotainer carboys (Nalgene). All plasticware was soaked with 10% HCl and flushed with Milli-Q water prior to use.

We chose four CRAM proxy compounds of varying molecular weights, including deoxycholate (414.55 Da) (Sigma-Aldrich D6750), humic acid (6.80–30.40 kDa) (Sigma-Aldrich 53680), lignin polymers (1.44–78.40 kDa) (Sigma-Aldrich 370959), and benzoic acid (molecular weight 122.12 Da) (Sigma-Aldrich 242381) (Perminova et al. 2003; Tolbert et al. 2014). Deoxycholate is a steroid; lignin is a major structural component common to vascular plants; humic acids are a mixture of organic heteropolycondensates; and benzoic acid is an aromatic compound present in plants and animals (Fig. S1).

Humic acid, lignin, and benzoic acid are insoluble in water; thus, they were dissolved in a pH 9 sodium hydroxide solution and then filtered through a combusted GF/F and a 0.2 μm polycarbonate filter for preparation of stock solutions. Deoxycholate was dissolved in Nanopure water. DOC concentrations of stock solutions were quantified and stock solutions were amended into the replicate seawater cultures with an amended target DOC concentration of 10 μmol C L^{-1} (actual measured concentrations varied between 4.27 μmol C L^{-1} and 11.09 μmol C L^{-1}, with differences explained by compound precipitation that

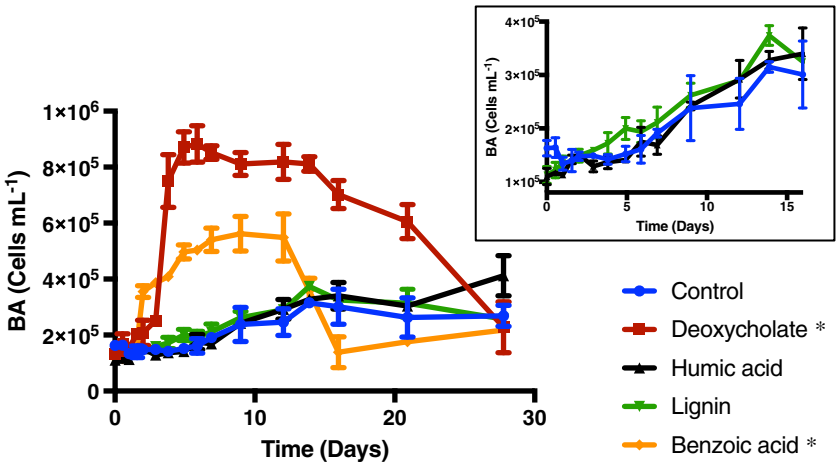

Fig. 1. Change of total bacterioplankton abundance (BA) with time for each treatment. Data are presented as average ± standard deviation of the replicate incubations. Inset shows the enlarged plot of BA from 0 d to 16 d for the control, humic acid, and lignin treatments. Deoxycholate and benzoic acid significantly differed from control (indicated as asterisk).

occurred during the freezing and thawing process between storage and amendment, or possible sorption to the carboy walls). The pH change due to the addition of pH 9 sodium hydroxide was negligible (<0.0009 pH units), because less than 13 mL stock solution was amended in the individual 5.5 L carboys. An unamended control treatment was prepared and all cultures were placed into an environmental chamber and incubated in the dark at the in situ temperature of 19.7°C for 28 d (initiated onboard the R/V *Atlantic Explorer* and then continued at the Bermuda Institute of Ocean Sciences after the cruise). These experiments were designed to assess bacterioplankton growth during exponential growth phase (i.e., days), before top-down processes begin to impact the community. DOM remineralization was measured over both the short (days) and long (weeks) duration. Samples for bacterioplankton abundance (BA), DOC concentration, fluorescence in situ hybridization (FISH) or catalyzed reporter deposition (CARD)-FISH, DNA, total combined dissolved amino acid (TDAA) and DOM composition (high-resolution DOM, HR-DOM) were drawn throughout the incubation (Figs. 1 and 2).

Incubation subsampling

To minimize sample handling and reduce the possibility of DOC contamination, all subsampling was carried out using a custom positive-pressure system to enable subsampling without removing caps from the biotainers. An aquarium pump pumped air through a hydrocarbon trap, which pressurized the biotainers and displaced sample water through submerged Teflon tubing into collection bottles (Fig. S2).

BA samples (10 mL aliquots) and FISH or CARD-FISH samples (45 mL aliquots) were fixed with 0.2 μm filtered formaldehyde (1% final concentration), stored at 4°C and processed within 48 h or stored at −80°C. DOC samples (duplicate 30 mL aliquots) were filtered through double stacked GF-75 filters (Advantec, pore size 0.3 μm, precombusted), packed in 25 mm Swinnex filter holders attached directly to the sample line with a Luer lock adaptor, and collected into 40 mL precombusted EPA glass vials with polytetrafluoroethylene (PTFE) coated silicone septa. DOC samples were acidified with 60 μL 4 N HCl to pH 3. TDAA samples were filtered through the same filters into 60 mL acid-washed high-density polyethylene (HDPE) bottles and stored at −20°C. DNA samples and HR-DOM samples for liquid chromatography coupled to FTICR-MS analysis were only sampled at 0 d and 5 d due to water budget constraints. One liter of seawater combined as 0.5 L from each duplicate biotainer was filtered through an Omnipore PTFE filter (pore size 0.2 μm, dia. 47 mm, Millipore) in a perfluoroalkoxy (PFA) filter holder into a PFA bottle. DNA filters were stored at −80°C until extraction, and 1 L filtrate was acidified with 1 mL ultrapure HCl (Optima, 35%) to pH ~3, stored at 4°C and processed within 24 h.

Sample analyses

BA samples were stained with 5 μg mL^{-1} 4′, 6-diamidino-2-phenylindole dihydrochloride (DAPI, Sigma-Aldrich) and enumerated with an Olympus AX70 epifluorescence microscope under ultraviolet excitation (Porter and Feig 1980) at 1000× magnification. This method cannot differentiate between bacteria and archaea; thus, the combined cell counts are hereafter referred to as bacterioplankton abundance. Cell biovolume was determined from 10 images captured with a digital camera (Retiga Exi-QImaging, Surrey, BC, Canada). Images were processed using ImageJ software according to established image analyses protocols (Baldwin and Bankston 1988; Sieracki et al. 1989). Bacterial carbon (BC) was calculated as BC = BA × cell biovolume × carbon conversion factor of 148 fg C μm^{-3}, associated with Sargasso Sea bacterioplankton (Gundersen et al. 2002).

DOC was analyzed using high-temperature combustion method on a modified TOC-V or TOC-L analyzer (Shimadzu) at the University of California, Santa Barbara as described in Carlson et al. (2010). The precision for DOC analysis is ~ 1 μmol L^{-1} or a CV of ~2%. Daily reference waters were

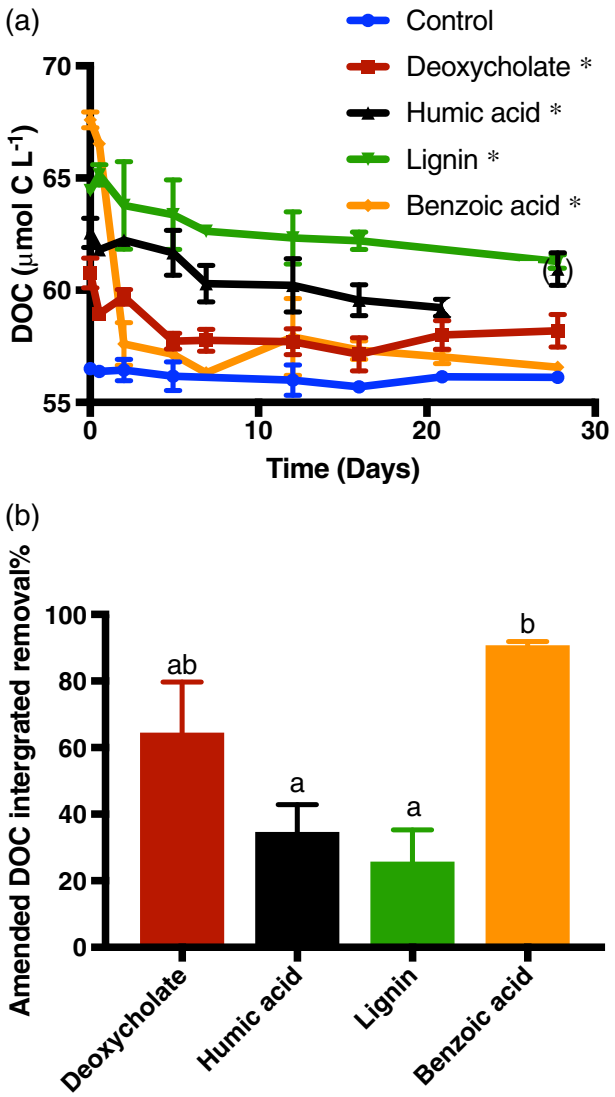

Fig. 2. **(a)** DOC concentration changes with time for each treatment (DOC for humic acid on 28 d was contaminated, thus data are shown in bracket and excluded for the following analysis). All treatments significantly differed from control (indicated as asterisk). **(b)** Percentage of amended DOC (T0 DOC in amendments minus T0 DOC in control) removed (based on integrated DOC removal, Fig. S3) over 20–28 d in the amendments. Data are presented as average ± standard deviation of the replicate incubations. Different letters above bars indicate significant difference between treatments at the α = 0.05 level.

calibrated with DOC CRM provided by D. Hansell (University of Miami).

FISH and CARD-FISH samples were filtered onto a 0.2 μm polycarbonate filter (Osmonics) and hybridized with Cy3-labeled probes targeting the bacterial lineages of SAR202, SAR11, *Alteromonas*, *Roseobacter* and the archaeal lineages of Euryarchaeota, and Thaumarchaeota (Table S1). SAR202, *Alteromonas*, and *Roseobacter* were quantified using FISH (Morris et al. 2002; Morris et al. 2004; Parsons et al. 2012; Parsons et al. 2015), while SAR11, Euryarchaeaota, and Thaumarchaeaota were enumerated using CARD-FISH (Teira et al. 2004; Herndl et al. 2005; Parsons et al. 2015). A nonsense probe 338F-Cy3 was used as the negative control for FISH and Non338-Cy3 was used as the negative control for CARD-FISH. Detailed hybridization parameters and protocols are described in Parsons et al. (2015) and in Table S1.

DNA was extracted from filters using the phenol chloroform protocol described in Giovannoni et al. (1996). Genomic DNA was amplified with the forward primer 27F (5′-AGAGTTTGATC NTGGCTCAG-3′) and the reverse primer 338RPL (5′-GCW GCCWCCCGTAGGWGT-3′) with "general" Illumina overhang adapters. Libraries were pooled in equimolar concentrations prior to sequencing. Samples were sequenced using one 2 × 250 Paired-End lane with a MiSeq Reagent Kit v2 at the Center for Genome Research and Biocomputing (Oregon State University), Corvallis, Oregon. Sequence data were trimmed, dereplicated, checked for chimeras, and assigned to taxonomies using the DADA2 R package, version 1.2 (Callahan et al. 2016) and with the phylogenetic taxonomic assignation program, PhyloAssigner (Vergin et al. 2013).

Replicate TDAA samples were dried by Speedvac (Savant SC210A) and then hydrolyzed by 6 N HCl (with 1% 12 mmol L^{-1} ascorbic acid to prevent oxidation of amino acids by nitrate) under nitrogen at 110°C for 20 h (Henrichs 1991; Kuznetsova and Lee 2002). Hydrolysate was filtered through combusted quartz wool and neutralized via evaporation under nitrogen. Nanopure blanks followed the same extraction protocol as samples. Amino acids were analyzed by high performance liquid chromatography (HPLC, Dionex ICS 5000+) equipped with a fluorescence detector (Dionex RF2000, Ex = 330 nm, Em = 418 nm) after precolumn *o*-phthaldialdehyde derivatization (Lindroth and Mopper 1979; Kaiser and Benner 2009; Liu et al. 2013). Phenylalanine (Phe) peaks overlapped with an unknown peak in our seawater samples and could not be differentiated from the background peak. Because Phe typically accounts for <3% of TDAA in the oligotrophic Sargasso seawater (Keil and Kirchman 1999; Kaiser and Benner 2009), Phe was excluded from the following data analysis.

Acidified HR DOM samples were passed through Bond Elut PPL cartridges (Agilent, 1 g/6 mL) to extract extracellular DOM. Extraction followed the protocol of Dittmar et al. (2008) with modifications as described in Longnecker (2015). Extraction efficiency for marine DOC using PPL cartridge is 43–62% (Dittmar et al. 2008; Johnson et al. 2017). Extracted DOM were analyzed using untargeted mass spectrometry methods described in Kido Soule et al. (2015). Mass-to-charge (*m/z*) ratios, retention times, and peak areas were measured for each sample. Here, we will use the term "mzRT features" to refer to chemical features with unique combinations of *m/z* values and retention times.

Data analysis and statistics

Bacterioplankton specific growth rates (μ) were calculated as the slope of ln(BA) vs. time during the exponential growth

phase of each treatment (Table 1). Stationary phase was reached at different times for each treatment and was determined using the growthcurver package in R (Sprouffske 2018) as $2 \times t_{mid}$, where t_{mid} is the time when BA reached half carrying capacity assuming a logistic growth model. BC and DOC at the calculated stationary time point were interpolated if sampling did not coincide with the modeled estimate of stationary phase. To maximize the use of all available data, we derived bacterial growth efficiency (BGE) from the ratio of the integrated area under the BC curve to the integrated area of the DOC removal curve:

$$BGE = \frac{\int_{T0}^{Tstationary} BC\, dt}{\int_{T0}^{Tstationary} DOC\, dt}$$

where t represents time, ∫BC represents the time normalized integrated area under the growth curve from T0 to stationary phase and ∫DOC represents time-normalized area under the DOC removal curve (see example in Fig. S3). Note that the integrated area here refers to the area under the curve of discrete data points using the integrateTrapezoid function in R.

Repeated measures ANOVA of the BA and DOC curves was used to assess difference ($p < 0.05$) between treatments and time points (Fit Model in JMP 13 Pro). Probe data were sampled less frequently than BA and DOC data and did not meet the criteria for repeated measures ANOVA. Thus, probe data (time normalized integrated area under probe abundance curve) for each treatment were compared to the control treatment at its corresponding time point of maximal abundance using *t* test (α = 0.05). Difference of integrated DOC percent removal among amendments was tested with ANOVA and Tukey's multiple comparison test (α = 0.05).

Bacterial community structure inferred from the 16S rRNA gene was plotted using phyloseq, vegan, and ggplot2 package in R (Oksanen et al. 2007; McMurdie and Holmes 2013). DNA from the humic acid and benzoic acid treatments did not amplify, possibly due to inhibition during PCR; thus, bacterial community structure data are only presented for the control, deoxycholate, and lignin treatments.

Principal component analysis (PCA) was conducted on mol% of amino acid composition (Xue et al. 2011). Amino acid data were first standardized (deviation from mean divided by standard deviation) before analysis to eliminate skew of PCA loading weight on dominant amino acids in samples. The mzRT features were grouped into compound classes based on the elemental formulas and the calculated aromaticity index (AI_{mod}) as corrected in Koch and Dittmar (2016). The following groups were defined by Martínez-Pérez et al. (2017) and Hertkorn et al. (2006): black carbon, polyphenols, highly unsaturated compounds, unsaturated aliphatic compounds, peptides, sugars, saturated fatty acids, and CRAM.

Table 1. Bacterial specific growth rate (μ, average ± standard deviation of replicates), ∫ bacterioplankton abundance (integrated under BA growth curve and time normalized), ∫ bacterial carbon (integrated under growth curve and time normalized, based on BA, cell biovolume and carbon conversion factor, assuming a carbon conversion factor of 148 fg C μm^{-3} [Gundersen et al. 2002]), ∫ DOC (integrated under DOC removal curve and time normalized) and bacterial growth efficiency (BGE), BGE = ∫ BC dt/∫ DOC dt (Carlson and Hansell 2015) over relevant time points.

	Specific growth rate		BGE				DOC bioavailability			
Treatments	Exponential time points	μ specific growth rate (d^{-1})	Initial to stationary time points	∫ BA (cells mL^{-1})	∫ BC (μmol C L^{-1})	∫ DOC (μmol C L^{-1})	BGE (%)	∫ DOC_{2d} (μmol C L^{-1})	∫ DOC_{5d} (μmol C L^{-1})	∫ DOC_{12d} (μmol C L^{-1})	∫ DOC_{28d} (μmol C L^{-1})
Control	4–14 d	0.08 ± 0.01	0–18.8 ± 3.1 d	$5.7\times10^4 \pm 3.5\times10^4$	0.12 ± 0.08	Nr*	-	Nr	Nr	Nr	Nr
Deoxycholate	1–4 d	0.51 ± 0.02	0–6.6 ± 0.3 d	$3.8\times10^5 \pm 1.8\times10^3$	0.73 ± 0.37	2.10 ± 0.82	34 ± 4	1.30 ± 0.83	1.75 ± 0.94	2.51 ± 0.79	2.79 ± 1.11
Humic acid	4–14 d	0.10 ± 0.01	0–18.5 ± 1.6 d	$1.2\times10^5 \pm 8.2\times10^3$	0.18 ± 0.04	1.95 ± 0.68	10 ± 6	Nr	Nr	1.47 ± 0.86	2.10 ± 0.76
Lignin	2–14 d	0.08 ± 0.01	0–15.2 ± 3.7 d	$1.2\times10^5 \pm 1.2\times10^3$	0.20 ± 0.06	1.48 ± 0.85	14 ± 4	Nr	Nr	1.27 ± 1.09	2.01 ± 0.79
Benzoic acid	1–5 d	0.38 ± 0.11	0–5.0 ± 1.1 d	$1.9\times10^5 \pm 3.0\times10^4$	0.60 ± 0.07	7.73 ± 1.37	8 ± 1	4.18 ± 0.63	7.76 ± 0.73	9.43 ± 0.13	10.02 ± 0.15

*Not resolvable (< 1 μmol C L^{-1}).

Results

Bacterial growth among treatments

Microbial response curves were typical of logistic growth, but the response for each treatment varied in terms of maximal cell density, duration of log phase (exponential phase), μ and time until reaching stationary phase (Fig. 1, Table 1). There was significant difference of BA among treatments ($p < 0.0001$) and among time ($p = 0.0030$), but no significant difference in the interaction between treatment and time ($p = 0.4962$). Bacterioplankton response was greatest in the deoxycholate treatment, followed by the benzoic acid, both significantly different from the control ($p = 0.0002$ and $p = 0.0084$, respectively). The μ measured in the deoxycholate and benzoic acid treatments were 4–5 times greater than the control (Table 1). Cell biovolumes in the deoxycholate and benzoic acid treatments were greatest among all treatments (Table S2) and dominated by rod-shaped cells (Fig. S5).

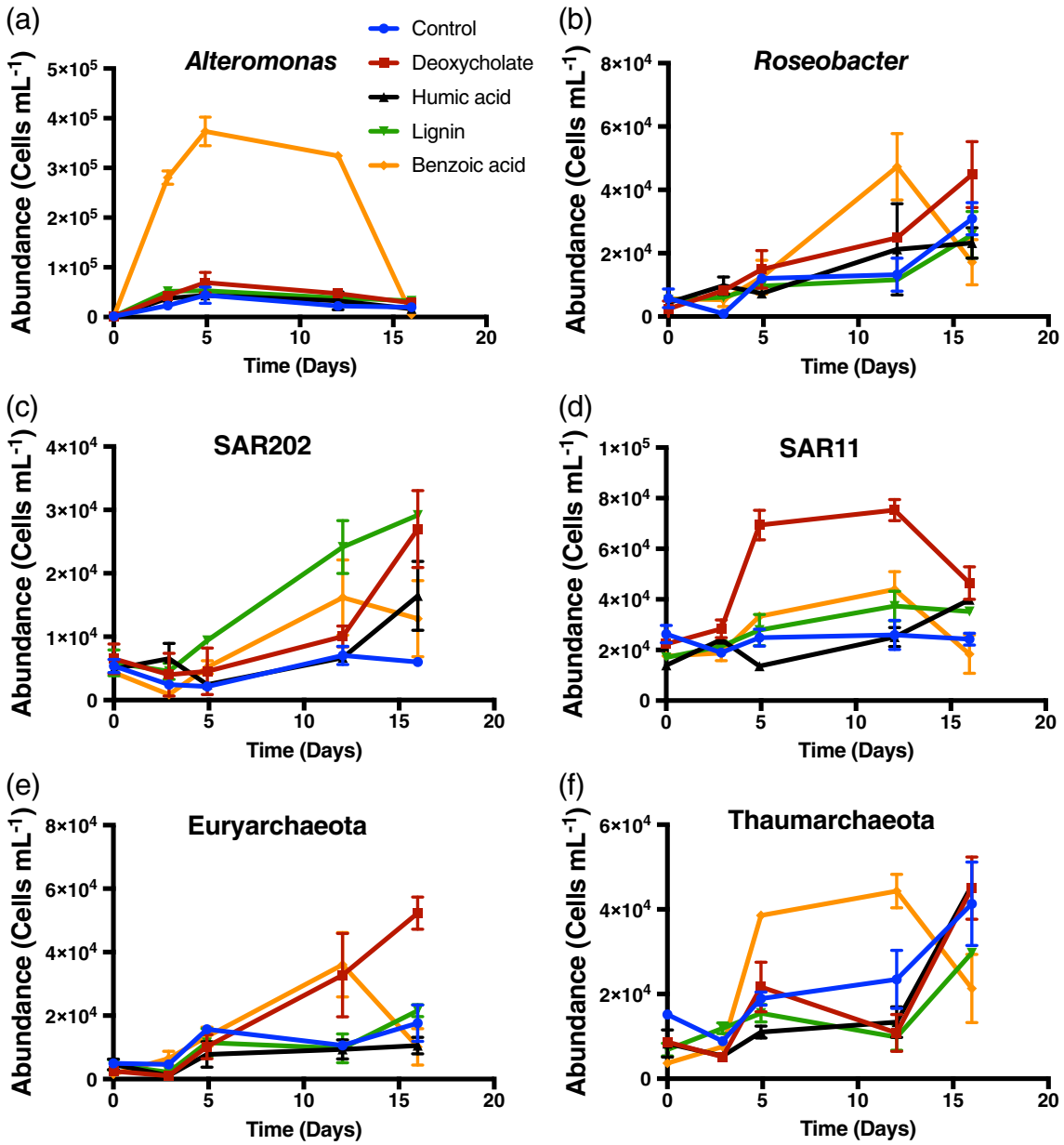

Fig. 3. Abundance of targeted bacterial and archaeal lineages over time, including **(a)** *Alteromonas*, **(b)** *Roseobacter*, **(c)** SAR202, **(d)** SAR11, **(e)** Euryarchaeota, and **(f)** Thaumarchaeota, detected by FISH and CARD-FISH. Note y axis scales are different for each lineage. Data are presented as average ± standard deviation of the replicate incubations.

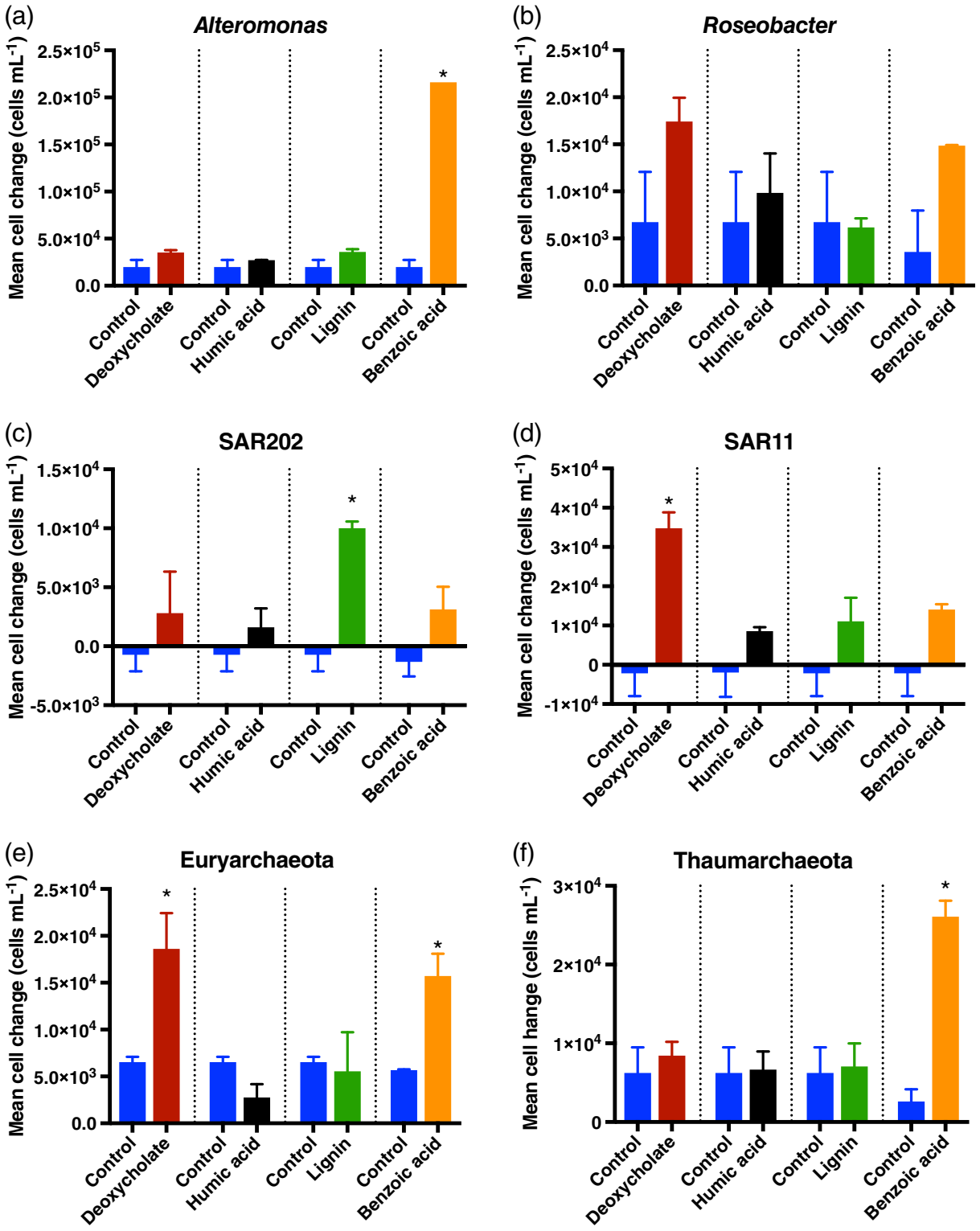

Fig. 4. Mean cell change (integrated and time normalized change in abundance when abundance of each lineage reached maximum) of targeted bacterial and archaeal lineages in amendments and control at corresponding time points (Fig. 3). As the various treatments reached maximum at different time points, multiple bars of control were provided at corresponding time for comparison with amendments. Data are presented as average ± standard deviation of the replicate incubations and asterisks indicate significant change in treatments (*t* test, $p < 0.05$).

In contrast to the rapid growth observed in the deoxycholate and benzoic acid treatments, growth in the control, humic acid, and lignin treatments was slow and reached stationary phase 10–14 d later (Fig. 1, Table 1). BA responses in the humic acid and lignin treatments were systematically greater than the control (i.e., ∫BA over same time was twofold greater than the control, Table 1), but were not statistically different from the control (Fig. 1). The μ in the lignin and

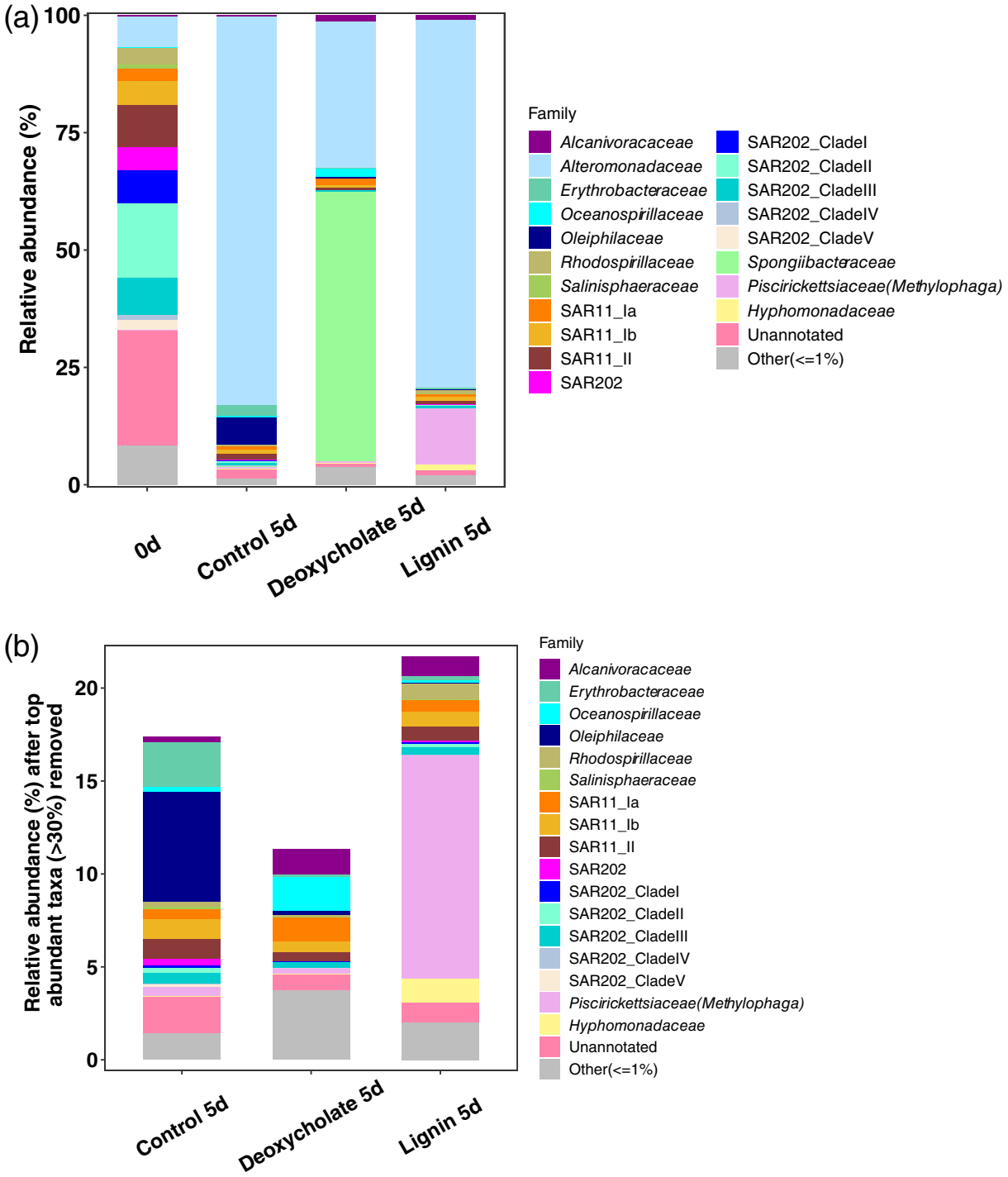

Fig. 5. **(a)** Change of bacterial community structure (at family level) with time via 16S rDNA phylogeny in the control, deoxycholate, and lignin treatments. DNA from the humic acid and benzoic acid treatments were not amplified due to inhibitors. **(b)** Bacterial community structure (at family level) via 16S rDNA phylogeny after removing the top most abundant taxa (>30%, *Alteromonadaceae* and *Spongiibacteraceae*) from the control, deoxycholate, and lignin treatments.

humic acid treatments were similar to that of the control (Table 1).

DOC removal and BGE in all treatments

DOC concentration for humic acid on day 28 increased by 1.73 μmol L^{-1}, was considered contaminated, and thus the data were excluded from further analysis. Change in DOC concentration was different among treatments ($p < 0.0001$) and over time ($p = 0.0006$), with no significant difference on the interaction between treatment and time ($p = 0.1189$) (Fig. 2a). DOC removal was significant for all amendment treatments over the course of the incubation ($p < 0.0001$ for deoxycholate, humic acid, lignin, and $p = 0.0476$ for benzoic acid), in contrast to the non-resolvable (< 1 μmol C L^{-1}) change observed in the control. DOC removal was most pronounced over the first 5 d in the deoxycholate and benzoic acid treatments and remained

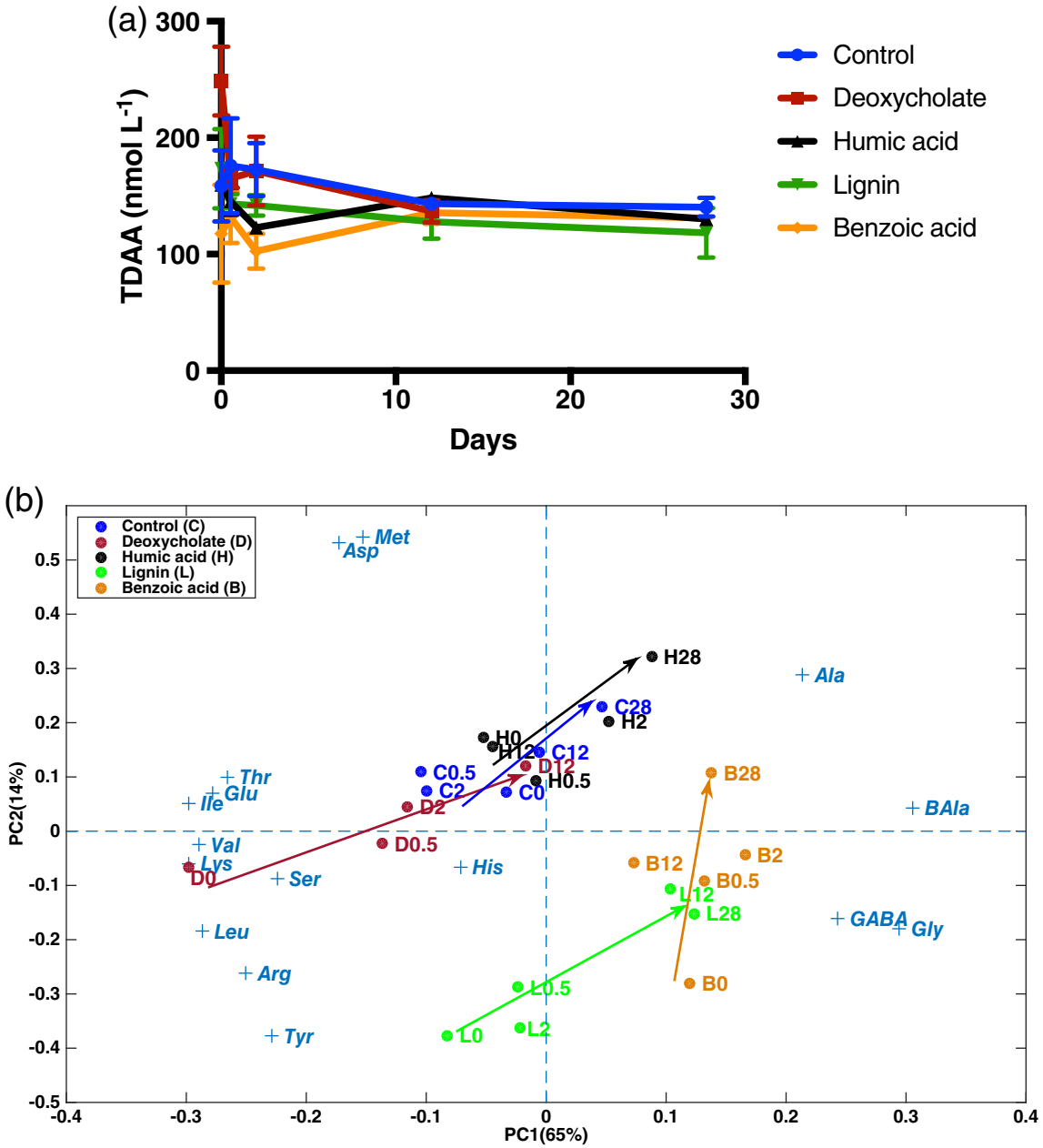

Fig. 6. **(a)** TDAA concentrations over incubation time for each treatment. Data are presented as average ± standard deviation of the replicate incubations. **(b)** Principal component analysis of TDAA composition data as molar percentages in five treatments for different time points (numbers are days). Data of deoxycholate 28 d samples were excluded due to sample contamination. Asp, aspartic acid; Glu, glutamic acid; His, histidine; Ser, serine; Arg, arginine; Thr, threonine; Gly, glycine; BAla, β-alanine; Tyr, tyrosine; Ala, alanine; GABA, γ-aminobutyric acid; Met, methionine; Val, valine; Ile, isoleucine; Leu, leucine; Lys, lysine. Arrows indicate overall amino acid compositional shift toward right and top corner for each treatment.

unchanged afterward (Fig. 2, Table 1). Almost all amended DOC was degraded in the benzoic acid treatment within 2 d. The percent removal of DOC relative to amended concentrations (T0 DOC in amendments minus that in control) was greatest in the benzoic acid treatments (90%), followed by deoxycholate treatment (64%) (Fig. 2b). DOC removal was gradual and linear throughout the entire incubation for the humic acid and lignin treatments with removal of amended concentrations equivalent to 34% and 25%, respectively (Fig. 2, Table 1). BGE was greatest in the deoxycholate treatment and lowest in the benzoic acid treatment (Table 1), indicating that different carbon and energy allocation strategies were used by the responding bacterioplankton between treatments.

Response of specific bacterial and archaeal lineages to amendments

Copiotroph response

Response by *Alteromonas* and *Roseobacter* was most pronounced in the benzoic acid and deoxycholate treatments (Figs. 3 and 4). *Alteromonas* dominated in the benzoic acid treatment, accounting for up to 75% of total BA and was significantly different from the control (Figs. 3a, 4a, and S6a). The abundance of *Alteromonas* reached a maximum by day 5 and decreased precipitously after day 12. Changes of *Roseobacter* in the amended treatments were not significantly different from that in the control (Figs. 3b and 4b).

Oligotroph response

Production of members of the SAR202 clade was greater in all CRAM proxy amendments compared to the control, and was most pronounced and significant for the lignin treatment (Fig. 3c and 4c). Cell densities for SAR202 increased three- to five-fold for the amendment treatments, compared to the control. The relative contribution of SAR202 to total cell abundance increased from 3% to 5% to a maximum of 4% to 9% for the amended treatments (Fig. S6). SAR11 increased in all amendments and its production was greatest in the deoxycholate treatment (Figs. 3d and 4d). Despite the significant increase of SAR11 cell abundance in the deoxycholate treatment, the relative contribution of SAR11 actually decreased over time due to the larger increase in other bacterioplankton lineages (Fig. S6b).

Archaeal response

Production of Euryarchaeota was greatest in the benzoic acid and deoxycholate treatments, with a twofold increase in cell abundance relative to the control (Figs. 3e and 4e). Production of Thaumarchaeota was observed in all treatments including the control and was greatest early in the benzoic acid treatment. The maximum change of Tharmarchaeota in the benzoic acid treatment was significantly different from that in the control (Figs. 3f and 4f).

Bacterial community structure changes during the incubation

A substantial proportion of the bacterioplankton response was comprised of lineages not detected by targeted FISH or CARD-FISH probes in the deoxycholate treatment at 5 d (Fig. S6). 16S rDNA amplicon sequencing and bacterial community structure analysis revealed that 58% of the sequenced community was comprised of the Gammaproteobacteria *Spongiibacteraceae* (Fig. 5a). It should be noted that the bacterial community structure data from DNA sequencing are expressed as relative percentage after PCR amplification. Thus, if taxa have unequal gene copy numbers, the data would not be directly comparable to the absolute percentage based on cell counts from the probe analysis. Bacterial community structure in the control treatment changed from a diverse composition of SAR11, SAR202, *Alteromonodaceae*, and SAR406 to one dominated by *Alteromonodaceae* by 5 d. This may be attributed to bottle effects resulting from cell stress in confined environments, cell binding on container surface, biofilm formation or introduction of trace organic nutrients (Lee and Fuhrman 1991; Fletcher 1996; Stewart et al. 2012). Bottle effects often select for growth of

Table 2. Bulk LC-FTICR-MS parameters of dissolved organic compounds at 0 d and 5 d for each treatment. Elemental ratios were calculated as magnitude-averaged values (Sleighter and Hatcher 2009) for mzRT features with assigned elemental formulas.

Sample ID	# mzRT features	# elemental formulas	$H:C_w$	$O:C_w$	DBE_w*
Control-0 d	1864	953	0.71	0.23	5.61
Control-5 d	1863	974	0.90	0.23	5.64
Deoxycholate-0 d	1995	1025	1.14	0.14	5.05
Deoxycholate-5 d	1858	954	0.67	0.21	5.41
Humic acid-0 d	1831	977	0.76	0.25	6.01
Humic acid-5 d	1842	951	0.82	0.24	5.89
Lignin-0 d	1873	964	0.73	0.23	5.88
Lignin-5 d	1896	980	0.76	0.23	5.77
Benzoic acid-0 d	1832	946	0.71	0.24	5.80
Benzoic acid-5 d	1861	952	0.82	0.23	5.69

*DBE (Double Bond Equivalent) = (2 + 2*C-H + N + P)/2.

Gammaproteobacteria (Eiler et al. 2000; Dinasquet et al. 2013; Muller et al. 2018), which is consistent with the increased relative contribution of *Alteromonadaceae* amplicons in our control treatment. Alternatively, high percentage of *Alteromonadaceae* at 5 d in the control may be due to bias in the amplicon yield based on increased gene copy numbers associated with this r-strategist (Alon et al. 2011; Gonzalez et al. 2012; Math et al. 2012).

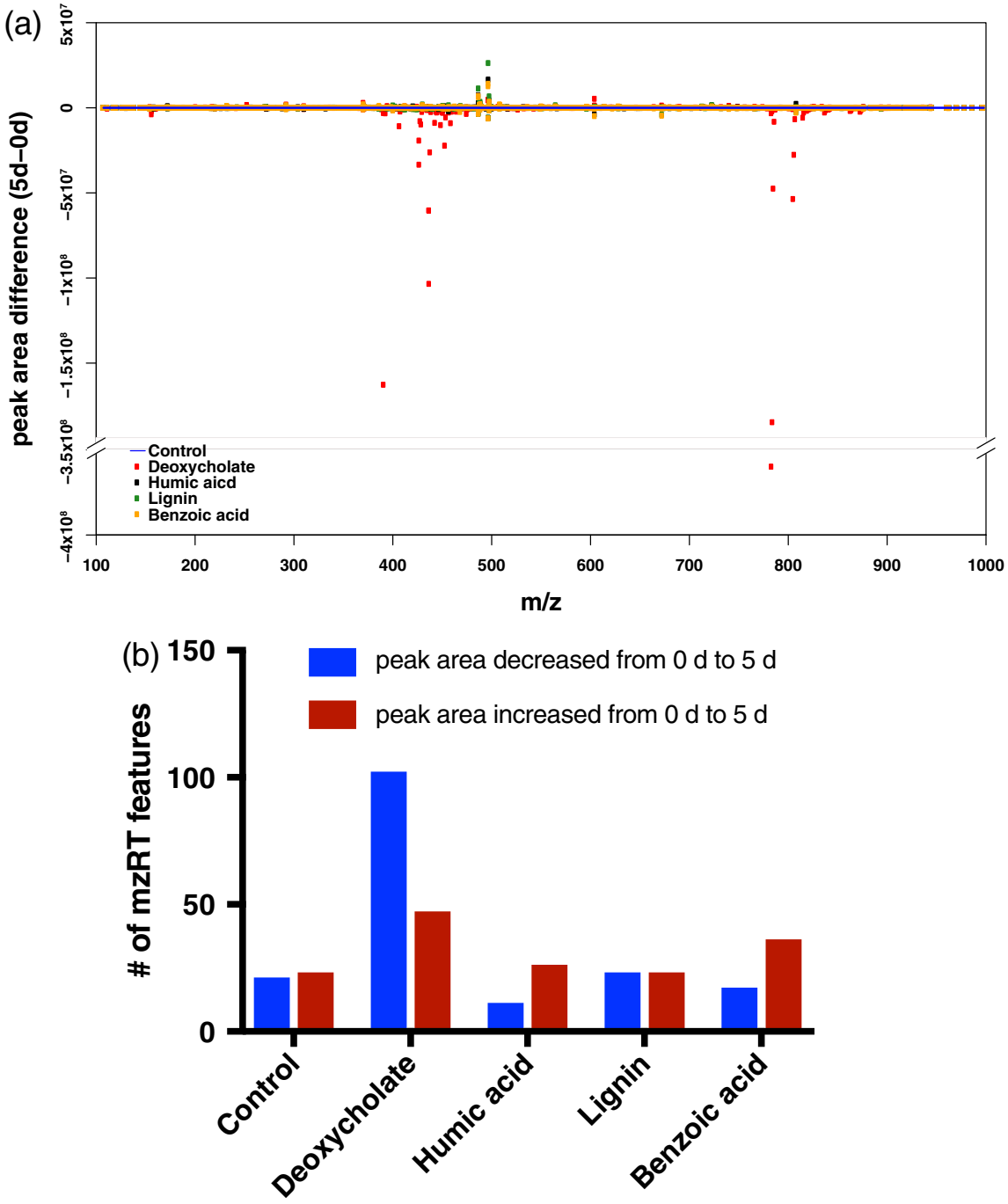

Fig. 7. (a) Difference in peak areas from 0 d to 5 d in treatments for each mzRT feature detected through LC-FTICR-MS. The blue line is the mean value of peak area difference for control. Points are color-coded by treatments. Any points with positive values are instances where the peak area increased from 0 d to 5 d, negative values are instances where the peak area decreased from 0 d to 5 d. **(b)** The number of mzRT features that had a difference in peak area that exceeds the difference measured in the control (features that were greater than the mean in the control plus one standard deviation or less than the mean in the control minus one standard deviation were deemed noteworthy). In blue are the mzRT features that decreased from 0 d to 5 d, in red are the mzRT features that increased from 0 d to 5 d.

In order to resolve the signal of lower contributing taxa, taxa accounting for >30% (*Alteromonadaceae* and *Spongiibacteraceae*) were removed from the plot and bacterial community structure at day 5 was compared again. SAR11 Ia was more enriched in the deoxycholate treatment than in the control at day 5 (Fig. 5b), consistent with the growth of SAR11 as shown in the probe data (Fig. 3d). *Alcanivoracaceae* and *Oceanospirillaceae* also became more enriched in the deoxycholate treatment than in the control at day 5.

The relative abundance of *Alcanivoracaceae*, *Piscirickettsiaceae* (specifically the genus *Methylophaga*), and *Hyphomonadaceae* increased with time in the lignin treatment, reaching 1%, 12%, and 1.3% respectively at 5 d, in contrast to 0.3%, 0.5%, and 0.04% in the control (Fig. 5). At day 5 in the lignin treatment, SAR202 were still in the early exponential phase (Fig. 3c); thus, their relative abundance in the DNA profile was small (Fig. 5).

TDAA concentrations and compositions throughout the incubation

Concentrations of TDAA decreased rapidly in amendments during the first 2 d (Fig. 6a). The %molar composition of TDAA clustered according to treatment type, then within each treatment, the trajectory of the %molar fraction TDAA shifted from the lower left quadrant toward the upper right quadrant of the PCA biplot (arrows in Fig. 6b) throughout the incubation. The lower left quadrant of the PCA biplot was dominated by Val, Lys, Ser, Leu, Arg, Tyr, while upper right quadrant was dominated by amino acids β-alanine (BAla) and alanine (Ala), signifying a compositional change of these amino acids with incubation time, and thus, an indication of a diagenetic alteration with incubation time.

Patterns of mzRT features from LC FTICR-MS analysis

There were 1831–1995 mzRT features detected and among them, 951–1025 were assigned elemental formulas (Table 2). H:C and O:C ratios of these features indicate the compound saturation and oxidation state. The changes in the H:C and O:C ratios from day 0 to day 5 were greatest for the deoxycholate treatment. The H:C ratio decreased by almost half by day 5 in the deoxycholate treatment in contrast to a slight increase in H:C for all other treatments. The O:C ratio increased 1.5-fold in the deoxycholate treatment; however, no systematic pattern was observed in the other treatments. The deoxycholate treatment showed a greater than fivefold increase in double bond equivalent (DBE = [2 + 2*C-H + N + P]/2) values relative to the control.

Figure 7a shows the change in the area for each peak (as semi-quantitative index) resolved in FTICR-MS. The greatest decrease in peak area with incubation time occurred in the deoxycholate treatment (Fig. 7a). Changes of peak area in the deoxycholate treatment were mostly in two m/z regions: m/z of 390–470 and m/z of 770–820. In other amendment treatments, greater changes were associated with increasing peak area from 0 d to 5 d. Peak area increases in the humic acid, lignin, and benzoic treatment were around the m/z region of 500.

The numbers of mzRT features with decreasing peak area over 5 d in the deoxycholate treatment were more than double those in all other treatments (Fig. 7b). In contrast, more mzRT features increased in peak area with time for the humic acid and benzoic acid treatments (Fig. 7b), while the number increasing and decreasing in peak area from 0 d to 5 d were similar for the control and lignin treatments. Among all treatments, deoxycholate showed the greatest number of mzRT features with both increasing and decreasing peak areas.

When grouping mzRT features into categorized compound classes, highly unsaturated compounds that partially overlap with CRAM compounds and black carbon compounds contributed to the majority of classified compounds (Table S4). The change in the number of features belonging to each class were similar for each treatment between 0 d and 5 d with the exception of unsaturated aliphatic compounds, which decreased more than fivefold in the deoxycholate treatment.

Discussion

Bacterioplankton trophic strategies are often divided into broad categories defined as copiotrophs and oligotrophs (Polz et al. 2006; Lauro et al. 2009). Copiotrophs are typically r-strategists and respond rapidly to the input of a limiting nutrient. In contrast, oligotrophs are usually characterized as K-strategists that maintain continuous but slow growth and are seemingly better adapted to survival in nutrient-limiting environments (Klappenbach et al. 2000; Yooseph et al. 2010; Gifford et al. 2013), including labile organic matter limitation.

BGE in the amendment treatments ranged from 8% to 34% from T0 until stationary phase, falling within the range of 7–40% previously reported for bacteria grown on ambient DOC or labile amino acid, glucose, and algal lysate (Suttle et al. 1991), suggesting that a majority of the utilized organic carbon was respired by mesopelagic bacterioplankton. Varying BGEs among the treatments indicated distinct resource allocation strategies utilized by the responding bacterioplankton communities.

Based on patterns of DOC removal and BA increase, we can divide the response to the four CRAM proxy compounds into two broad categories: labile and recalcitrant. DOC removal and BA increase were most pronounced in the benzoic acid and deoxycholate treatments, with the rapid change of DOC and BA during the first 2–5 d (Fig. 1, Fig. 2); thus, we group the compounds benzoic acid and deoxycholate as labile DOM in terms of their bioavailability to Sargasso Sea mesopelagic bacterioplankton. In contrast, DOC removal and BA increase in the lignin and humic acid treatments were minimal and gradual over 28 d; thus, we categorize these model compounds as recalcitrant DOM. Here we examine the response of distinct bacterioplankton groups to the two categories of CRAM proxy compounds and subsequent DOM transformation in all treatments.

CRAM proxy compounds that selected for copiotrophs

Benzoic acid and deoxycholate selected for several copiotrophic bacterioplankton. In comparison to lignin and humic acid, benzoic acid and deoxycholate are low molecular weight compounds of 122 Da and 415 Da, respectively, which can be transported through membrane "porin" proteins that have an exclusion limit of ~600 Da (Weiss et al. 1991). The molecular size of these compounds may contribute to easier access, transport and use by some bacterioplankton.

Alteromonas

The rapid change of DOC concentration in the benzoic acid treatment was concomitant with the increase in BA and dominant growth of *Alteromonas* (Figs. 3 and 4). Members of *Alteromonas* are well-known copiotrophs that grow rapidly when labile organic substrates become available, such as freshly produced DOM associated with phytoplankton blooms (Romera-Castillo et al. 2011; Wear et al. 2015). They are ubiquitous Gammaproteobacteria that effectively compete for labile DOM for growth (DeLong et al. 2006; McCarren et al. 2010; Pedler et al. 2014; Sherwood et al. 2015). Some *Alteromonas* members are also hydrocarbon-degraders that can bloom in the presence of marine oil spills enriched in alkanes and aromatic compounds (Math et al. 2012; Redmond and Valentine 2012; Hu et al. 2017; Liu et al. 2017). Metabolism of the aromatic ring of benzoic acid might have promoted the rapid growth of *Alteromonas* that we observed.

Spongiibacteraceae

Deoxycholate selected for fast-growing *Spongiibacteraceae*. Deoxycholate is a sterol derivative and a conjugate base of bile acids, which are generally produced in eukaryotic cells or by cholesterol metabolism in some bacterial strains (Li et al. 2009; Kim et al. 2012). The predominant large rod-shaped cells observed in the deoxycholate treatment (Table S2) are consistent with cell morphology reported for *Spongiibacteraceae* (Hwang and Cho 2009; Jean et al. 2016; Fig. S5). *Spongiibacteraceae* belongs to newly reclassified *Cellvibrionales* order and have been categorized as oligotophs (Spring et al. 2015). However, their rapid growth in the present study suggests that members of the *Spongiibacteracea* clade can adopt an r-strategy, when provided with favorable particular substrates. Consistent with the present study, Spring and Riedel (2013) reported that *Cellvirbionales*, traditionally designated as oligotrophs, grew rapidly under nutrient-rich conditions. Some members of *Spongiibacteraceae* may be r-strategists, while others are K-strategists, and the r-strategists were playing a role in oxidizing deoxycholate. Metagenome analysis revealed steroid-degrading capability within *Spongiibacteraceae* (Holert et al. 2018), indicating a nutritional benefit from the uptake of sterols (Webster and Thomas 2016; Lengger et al. 2017).

Fast-growing archaea

Archaea in the Euryarchaeota and Thaumarchaeota (marine group I [MGI], previously Crenarchaeota) account for about one-third of the prokaryotic cells in the global ocean (Karner et al. 2001). While Thaumarchaeota are usually more abundant in deep water, Euryarchaeota, especially marine group II (MGII), can make up 2–22% of picoplankton abundance throughout the water column (DeLong et al. 1999; Herndl et al. 2005; Stoica and Herndl 2007; Zhang et al. 2009), which is consistent with the 3% Euryarchaeota contribution observed in our ambient seawater (Fig. S6). Euryarchaeota encode genes for transport of amino acids and oligopeptides, and protein degradation (Zhang et al. 2015; Lazar et al. 2017). MGII archaea are capable of utilizing organic molecules such as dissolved proteins, lipids, carbohydrates, and particulate organic matter (Iverson et al. 2012; Orsi et al. 2016; Xie et al. 2018). The observation of enhanced Euryarcheaota production in the deoxycholate and benzoic acid incubations implies that some lineages of Euryarchaeota are capable of metabolizing sterols and aromatic compounds.

Thaumarcheaota are chemoautotrophic ammonia-oxidizers that play an important role in nitrogen cycling (Konneke et al. 2005; Treusch et al. 2005). The enhanced production of Thaumarchaeota in the benzoic acid treatment may be indicative of a secondary response to ammonium produced during DOM mineralization by heterotrophic bacteria. Thaumarcheaota have been found in deep chlorophyll maxima and during the decline of phytoplankton blooms (Beman et al. 2011; Berg et al. 2018), suggesting an interactive role in organic matter remineralization and nutrient cycling. Coculture experiments have demonstrated enhanced Thaumarchaeota production in the presence of heterotrophic bacteria (Tourna et al. 2011), suggesting a potential interaction between bacteria and Thaumarchaeota. Alternatively, the growth of members of Thaumarcheaota in the benzoic acid treatment may be a consequence of mixotrophic utilization of organic carbon, which has been suggested by genomic studies (Hallam et al. 2006; Walker et al. 2010), contributing to their growth in the benzoic acid treatment.

Other bacteria

Copiotrophic *Oceanospirillaceae* and some typically oligotrophic bacterioplankton, including *Alcanivoracaceae* and SAR11, also became enriched in the deoxycholate treatment relative to the control (Figs. 5 and 3). However, it should be noted that their combined relative abundance was <10%. *Oceanospirillaceae* respond quickly to labile DOM released during phytoplankton blooms or to inorganic nutrient addition (Delmont et al. 2015; Goldberg et al. 2017; Hoffmann et al. 2017). The increase of *Oceanospirillaceae* in the deoxycholate treatment relative to the control was consistent with their copiotrophic role in labile DOM utilization.

CRAM proxy compounds that selected for oligotrophs

Of the proxy compounds, humic acid and lignin were the most resistant to microbial degradation, as indicated by the slow DOC removal and minimal changes in cell abundance. Lignin is derived from terrestrial plants and humic acid originates from

both terrestrial and marine sources. They are both polymers with complex chemical structures and are considered to be thermodynamically stable forms of carbon sources (Hedges et al. 1997; Mann et al. 2014). Although humic acid and lignin are relatively recalcitrant and tend to be resistant to rapid microbial degradation, some bacteria groups reportedly adapted to utilizing recalcitrant DOM appeared to respond to these CRAM proxy compounds. The bacterial response in the humic acid and lignin treatments included the oligotrophic SAR202, SAR11, *Alcanivoracaceae*, *Piscirickettsiaceae*, and *Hyphomonodaceae* rather than copiotrophic taxa. Our study is one of the few incubation studies able to show response by bacterial oligotrophs, rather than those typically categorized as copiotrophs, when amended with complex organic compounds. Despite slower growth rates (Fig. 1), the oligotroph response to the recalcitrant DOM was significant, indicative of their potential role in recalcitrant DOM oxidization.

SAR202

SAR202 bacteria, in the phylum *Chloroflexi*, are free-living heterotrophic bacterioplankton that contribute as much as 4–34% of total BA in the mesopelagic and bathypelagic realms of the Atlantic, Pacific, and Arctic Oceans (Morris et al. 2004; Morris et al. 2005; Schattenhofer et al. 2009; Lekunberri et al. 2013; Mehrshad et al. 2018). SAR202 accounted for 3–5% of the total BA and 39% of the 16S rRNA gene copies in the ambient 200 m mesopelagic water of Sargasso Sea, with subclades I, II, and III dominating the SAR202 group (Saw et al.) (Figs. S6 and 5a).

The significant growth response of SAR202 to lignin suggests that some SAR202 are capable of oxidizing this recalcitrant, CRAM-like polymeric compound. Bacterial and archaeal communities show a general trend of decreasing rates of L-aspartic acid (Asp) uptake while increasing rates of D-Asp uptake from subsurface to bathypelagic waters (Pérez et al. 2003; Teira et al. 2006). However, members of SAR202 can take up L-Asp at a constant rate throughout the water column with essentially no uptake of D-Asp (Varela et al. 2008). These uptake characteristics indicate that members of SAR202 are well adapted to scarce and patchy food resources and may be able to detect and exploit DOM not available to other bacterioplankton in the deep ocean.

Genomic and metagenomic sequences for SAR202 have revealed a variety of paralogous protein families capable of recalcitrant DOM catabolism. These include flavin mononucleotide/F420-dependent monooxygenases (FMNOs) that convert ketones to esters, dioxygenases that catalyze initial steps in aromatic ring catabolism, major facilitator superfamily (MFS) transporters, short-chain dehydrogenases that convert alcohols to ketones, and coenzyme A (CoA) transferases that catalyze the ATP-independent binding of carboxylic acids to CoA (Ridlon and Hylemon 2012; Landry et al. 2017; Thrash et al. 2017). These and other SAR202 enzymes may play roles in the oxidation of CRAM-like compounds such as humic acid and lignin.

SAR11

SAR11 are free-living aerobic heterotrophic Alphaproteobacteria that are distributed ubiquitously in the oceans, accounting for 15–40% of all planktonic cells throughout the water column (Morris et al. 2002; Rappe et al. 2002; Eiler et al. 2009; Schattenhofer et al. 2009) and comprise up to 47% of total bacterial 16S rRNA genes in oceanic samples (Sperling et al. 2012). In the present study, SAR11 group accounted for ∼15% of mesopelagic BA and ∼15% of 16S rRNA gene copies at T0 of the incubations (Figs. 5b and S6). Enhanced SAR11 production in our amendment treatments suggests that some SAR11 ecotypes may be involved in the catabolism of some CRAM-like DOM. A large proportion of SAR11 membrane transporters are ATP-binding cassette (ABC) transporters, with high substrate affinity (Giovannoni et al. 2005; Alonso and Pernthaler 2006; Noell and Giovannoni 2019) that may facilitate the transport of the small compounds like deoxycholate.

SAR11 cells have been demonstrated to utilize a wide variety of labile DOM compounds as substrates (Giovannoni 2017). They have evolved into a variety of ecotypes that partition ocean niches by temperature and probably other factors that remain unidentified (Carlson et al. 2009; Brown et al. 2012; Vergin et al. 2013). SAR11 ecotype Ia, found in the surface water of oligotrophic systems, appears to be correlated to low macronutrient concentrations and elevated flux of labile DOM derived from photosynthesis. At BATS, ecotype Ib occurs throughout the mixed layer in the late spring, and in the region of the deep chlorophyll maximum during the summer. Ecotype II is most prevalent in the upper mesopelagic in the late spring as the water column restratifies and semi-labile DOM transported from the summer surface layer by winter mixing is remineralized (Carlson et al. 2009). In the present study, SAR11 Ia became enriched with the amendment of deoxycholate compared to the control treatment (Fig. 5b), consistent with its proposed role in labile DOM remineralization. Examination of the relative abundances of SAR11 ecotypes did not reveal differences between the lignin and control treatments at 5 d, possibly because SAR11 production was not great enough to be differentiated between treatments at this early stage of growth (Fig. 5b). Unfortunately, water budget constraints did not allow DNA samples to be collected at the later time points necessary to resolve differences in the ecotypes.

Other oligotrophs: Piscirickettsiaceae (Methylophaga), Hyphomonodaceae, and Alcanivoracaceae

The increased relative abundances of other oligotrophs, including members of *Piscirickettsiaceae (Methylophaga)*, *Hyphomonadaceae*, and *Alcanivoracaceae*, in the lignin treatment, compared to the control (0–5 d) (Fig. 5b), suggest they may be involved in the catabolism of CRAM-like compounds. *Methylophaga* belonging to *Piscirickettsiaceae* are marine Gammaproteobacteria (Ravenschlag

et al. 2001; Wang et al. 2018) that have been shown to utilize peptides, oil, one-carbon compounds, such as methanol and methylamine, and polyamines (Neufeld et al. 2007; Lu et al. 2015; Deng et al. 2018; Hamdan et al. 2018; Kamalanathan et al. 2018). Wilhelm et al. (2018) identified members of *Piscirickettsiaceae* as lignin-degrading bacteria using a stable isotope probing approach. Members of *Hyphomonadaceae* can persist in extreme oligotrophic conditions (Lee et al. 2007; Abraham et al. 2013), and can respond to phytoplankton-derived DOM (Goldberg et al. 2017). Our results suggest that they can also respond to lignin. *Alcanivoracaceae* includes oligotrophic bacterioplankton that have a narrow substrate spectrum that includes a few organic acids but no simple sugars (Yakimov et al. 1998; Kalscheuer et al. 2007). They are hydrocarbon degrading specialists (i.e., alkanes) that often dominate the bacterial community during oil spills (Schneiker et al. 2006; Terrisse et al. 2017). The aliphatic structures in deoxycholate and lignin may facilitate their utilization of these two CRAM-like compounds in our incubations.

Microbial transformation of CRAM proxy compounds

TDAA compositions in each treatment shifted from high mol% Val, Lys, Ser, Leu, Arg, and Tyr, toward more enriched with β-Ala with incubation time (Fig. 6b). Mol% of Val, Lys, Ser, Leu, Arg, and Tyr decrease with decreasing degradation index, suggesting a high mol% of these amino acids is a marker of fresh organic matter (Dauwe et al. 1999; Kaiser and Benner 2009). The increase of β-Ala and GABA, which are nonprotein amino acids, relative to protein amino acids commonly is used as an indicator of organic matter diagenesis (Cowie and Hedges 1994; Davis et al. 2009; Kaiser and Benner 2009). Increases in %β-Ala and/or %GABA may be due to partial decarboxylation of aspartic acid and glutamic acid (Whelan 1977; Lee and Cronin 1982). The observed shift from more % of fresh amino acids to higher % β-Ala through time in each treatment indicates subtle but non-negligible diagenetic alteration during our incubations, with deoxycholate and lignin showing the most pronounced transformation.

LC FTICR-MS analysis provides information on the changes of elemental composition and molecular formulas of thousands of SPE-extracted DOM compounds (m/z of 100–1000). In contrast to minimal change in other treatments, the decreased H:C ratio and increased O:C ratio and DBE of the detected mzRT features from 0 d to 5 d in the deoxycholate treatment (Table 2) indicate that DOM in the deoxycholate treatment was transformed to compounds of increased unsaturation and oxygen content; consistent with previous reports that these proxies are indicators of aged DOM (Flerus et al. 2012; Medeiros et al. 2015).

Highly unsaturated compounds, black carbon, and CRAM compounds dominated the DOM for all treatments (Table S4), a finding consistent with marine DOM composition (Martínez-Pérez et al. 2017; Schmidt et al. 2017; Kellerman et al. 2018). Phytoplankton exudates enriched in unsaturated aliphatic compounds accumulate in the surface water compared to mesopelagic waters (Medeiros et al. 2015), suggesting net removal of aliphatic compounds in the deeper waters. The number of unsaturated aliphatic compounds decreased by 33% in the deoxycholate treatment (Table S4). Little change in elemental composition was observed in the lignin and humic acid treatments. It is possible that other analytical modes could have revealed DOM transformation (Osterholz et al. 2015; Zark et al. 2017; Lu et al. 2018). However, it is likely that due to logistical water budget constraints, our collection of LC FTICR-MS samples at day 5 was too early in the growth phase to detect DOM transformation differences in the humic acid and lignin treatments. Benzoic acid molecule is small and outside the analytical window of LC FTICR-MS, precluding its resolution despite significant DOC drawdown in that treatment.

In contrast to direct infusion FTICR-MS, LC FTICR-MS analysis first separates compounds on an LC column before introduction via ionization source into the mass spectrometer. This approach can increase the number of identified peaks (Patriarca et al. 2018) and provide an additional peak intensity data (using peak area as an index of relative concentrations). Greater than 100 mzRT features decreased in peak area during the incubation in the deoxycholate treatment (Fig. 7) and were mainly in the m/z regions of 390–470 and 770–820 Da. In contrast, mzRT features with increasing peak area over time were dominant in the humic acid, lignin, and benzoic acid treatments and were found near m/z of ~ 500 Da. The mzRT features were categorized into compound classes (Table S4) but <2% could be classified into each group; thus the majority of compounds remain unidentified. Nevertheless, differences in mzRT between 0 and 5 d for all the amended treatments indicate that DOM was transformed over the course of the incubation. When comparing peak changes over time, the average m/z values of all depleted peaks (decreasing peak area) were 7–73 Da larger than enriched peaks (increasing peak area) (Table S5). These peak alterations suggest that small side-chain functional groups were lost during microbial metabolism of DOM. For example, a methyl group can be removed through demethylation, and CO_2 can be lost via decarboxylation. Similar to our results, small mass differences of 20–40 Da were detected between depleted molecular formulas and enriched peaks in incubations of estuarine and coastal DOM (Vorobev et al. 2018).

Conclusions and implications

Through incubations of CRAM proxy compounds in mesopelagic seawater from the Sargasso Sea, this study showed that deoxycholate and benzoic acid degraded rapidly and were more consistent with labile DOM properties, while humic acid and lignin were more recalcitrant to microbial remineralization, suggesting that not all CRAM-like substrates can be simply classified as recalcitrant DOM. The bioreactivity appears to be intricately associated with the activity of specific bacterioplankton taxa. While labile CRAM proxy

compounds mostly selected for fast-growing copiotrophs like members of *Alteromonas*, *Spongiibacteraceae*, and the archaea *Euryarchaeaota* and *Thaumarchaeota*, recalcitrant CRAM proxy compounds in our incubations selected for slow-growing oligotrophs, such as members of SAR202, *Piscirickettsiaceae*, *Hyphomonadaceae*, and *Alcanivoracaceae*, that appear to be capable of oxidizing more recalcitrant DOM. Our results also showed that DOM was transformed to more degraded components with lower H:C ratio, higher O:C ratio and DBE in the deoxycholate incubation. This study used individual compounds to mimic recalcitrant DOM and unravel interactions between bacterioplankton and DOM rich in carboxylated alicyclic molecules. The data showed the different response of bacterioplankton lineages to CRAM-like DOM with varying quality, implying potential catabolism strategies and niche specialization among bacterioplankton. This study also highlights the important role of oligotrophs, which are often understudied in incubation experiments, especially on recalcitrant carbon oxidation. The growth of oligotrophs provides experimental evidence to support the metabolic roles of those bacterioplankton revealed from previous genomic studies. In the future, mixtures of DOM compounds that are more representative of overall recalcitrant DOM pool in seawater, such as SPE extracted DOM, might be used to further investigate microbial response to natural complex recalcitrant DOM and potential degraders of recalcitrant DOM in the ocean.

References

Abraham, W. R., H. Lunsdorf, M. Vancanneyt, and J. Smit. 2013. Cauliform bacteria lacking phospholipids from an abyssal hydrothermal vent: Proposal of Glycocaulis abyssi gen. nov., sp. nov., belonging to the family Hyphomonadaceae. Int. J. Syst. Evol. Microbiol. **63**: 2207–2215. doi:10.1099/ijs.0.047894-0

Alon, S., F. Vigneault, S. Eminaga, D. C. Christodoulou, J. G. Seidman, G. M. Church, and E. Eisenberg. 2011. Barcoding bias in high-throughput multiplex sequencing of miRNA. Genome Res. **21**: 1506–1511. doi:10.1101/gr.121715.111

Alonso, C., and J. Pernthaler. 2006. Roseobacter and SAR11 dominate microbial glucose uptake in coastal North Sea waters. Environ. Microbiol. **8**: 2022–2030. doi:10.1111/j.1462-2920.2006.01082.x

Baldwin, W. W., and P. W. Bankston. 1988. Measurement of live bacteria by Nomarski interference microscopy and stereologic methods as tested with macroscopic rod-shaped models. Appl. Environ. Microbiol. **54**: 105–109.

Beman, J. M., J. A. Steele, and J. A. Fuhrman. 2011. Co-occurrence patterns for abundant marine archaeal and bacterial lineages in the deep chlorophyll maximum of coastal California. ISME J. **5**: 1077–1085. doi:10.1038/ismej.2010.204

Benner, R., and R. M. W. Amon. 2015. The size-reactivity continuum of major bioelements in the ocean. Ann. Rev. Mar. Sci. **7**: 185–205. doi:10.1146/annurev-marine-010213-135126

Berg, C., C. L. Dupont, J. Asplund-Samuelsson, N. A. Celepli, A. Eiler, A. E. Allen, M. Ekman, B. Bergman, and K. Ininbergs. 2018. Dissection of microbial community functions during a cyanobacterial bloom in the Baltic Sea via metatranscriptomics. Front. Mar. Sci. **5**: 55. doi:10.3389/fmars.2018.00055

Brown, M. V., and others. 2012. Global biogeography of SAR11 marine bacteria. Mol. Syst. Biol. **8**: 595. doi:10.1038/msb.2012.28

Callahan, B. J., P. J. McMurdie, M. J. Rosen, A. W. Han, A. J. A. Johnson, and S. P. Holmes. 2016. DADA2: High-resolution sample inference from Illumina amplicon data. Nat. Methods **13**: 581–583. doi:10.1038/nmeth.3869

Carlson, C. A., and D. A. Hansell. 2015. DOM sources, sinks, reactivity, and budgets, p. 65–126. *In* D. A. Hansell and C. A. Carlson [eds.], Biogeochemistry of marine dissolved organic matter. Academic.

Carlson, C. A., H. W. Ducklow, and A. F. Michaels. 1994. Annual flux of dissolved organic carbon from the euphotic zone in the northwestern Sargasso Sea. Nature **371**: 405–408. doi:10.1038/371405a0

Carlson, C. A., H. W. Ducklow, and T. D. Sleeter. 1996. Stocks and dynamics of bacterioplankton in the northwestern Sargasso Sea. Deep-Sea Res. Pt. II. **43**: 491–515. doi:10.1016/0967-0645(95)00101-8

Carlson, C. A., S. J. Giovannoni, D. A. Hansell, S. J. Goldberg, R. Parsons, and K. Vergin. 2004. Interactions among dissolved organic carbon, microbial processes, and community structure in the mesopelagic zone of the northwestern Sargasso Sea. Limnol. Oceanogr. **49**: 1073–1083. doi:10.4319/lo.2004.49.4.1073

Carlson, C. A., R. Morris, R. Parsons, A. H. Treusch, S. J. Giovannoni, and K. Vergin. 2009. Seasonal dynamics of SAR11 populations in the euphotic and mesopelagic zones of the northwestern Sargasso Sea. ISME J. **3**: 283–295. doi:10.1038/ismej.2008.117

Carlson, C. A., D. A. Hansell, N. B. Nelson, D. A. Siegel, W. M. Smethie, S. Khatiwala, M. M. Meyers, and E. Halewood. 2010. Dissolved organic carbon export and subsequent remineralization in the mesopelagic and bathypelagic realms of the North Atlantic basin. Deep-Sea Res. Pt. II. **57**: 1433–1445. doi:10.1016/j.dsr2.2010.02.013

Cowie, G. L., and J. I. Hedges. 1994. Biochemical indicators of diagenetic alteration in natural organic-matter mixtures. Nature **369**: 304–307. doi:10.1038/369304a0

Dauwe, B., J. J. Middelburg, P. M. J. Herman, and C. H. R. Heip. 1999. Linking diagenetic alteration of amino acids and bulk organic matter reactivity. Limnol. Oceanogr. **44**: 1809–1814. doi:10.4319/lo.1999.44.7.1809

Davis, J., K. Kaiser, and R. Benner. 2009. Amino acid and amino sugar yields and compositions as indicators of

dissolved organic matter diagenesis. Org. Geochem. **40**: 343–352. doi:10.1016/j.orggeochem.2008.12.003

Delmont, T. O., A. M. Eren, J. H. Vineis, and A. F. Post. 2015. Genome reconstructions indicate the partitioning of ecological functions inside a phytoplankton bloom in the Amundsen Sea, Antarctica. Front. Microbiol. **6**: 1090. doi: 10.3389/fmicb.2015.01090

DeLong, E. F., L. T. Taylor, T. L. Marsh, and C. M. Preston. 1999. Visualization and enumeration of marine planktonic archaea and bacteria by using polyribonucleotide probes and fluorescent in situ hybridization. Appl. Environ. Microb. **65**: 5554–5563. doi:10.1128/AEM.65.12.5554-5563.1999

DeLong, E. F., and others. 2006. Community genomics among stratified microbial assemblages in the ocean's interior. Science **311**: 496–503. doi:10.1126/science.1120250

Deng, W., L. Peng, N. Jiao, and Y. Zhang. 2018. Differential incorporation of one-carbon substrates among microbial populations identified by stable isotope probing from the estuary to South China Sea. Sci. Rep. **8**: 15378. doi:10.1038/s41598-018-33497-6

Dinasquet, J., T. Kragh, M. L. Schroter, M. Sondergaard, and L. Riemann. 2013. Functional and compositional succession of bacterioplankton in response to a gradient in bioavailable dissolved organic carbon. Environ. Microbiol. **15**: 2616–2628. doi:10.1111/1462-2920.12178

Dittmar, T., B. Koch, N. Hertkorn, and G. Kattner. 2008. A simple and efficient method for the solid-phase extraction of dissolved organic matter (SPE-DOM) from seawater. Limnol. Oceanogr. Methods **6**: 230–235. doi:10.4319/lom.2008.6.230

Eiler, H., J. Pernthaler, and R. Amann. 2000. Successsion of pelagic marine bacteria during enrichment: A close look at cultivation-induced shifts. Appl. Environ. Microb. **66**: 4634–4640. doi:10.1128/AEM.66.11.4634-4640.2000

Eiler, A., D. H. Hayakawa, M. J. Church, D. M. Karl, and M. S. Rappe. 2009. Dynamics of the SAR11 bacterioplankton lineage in relation to environmental conditions in the oligotrophic North Pacific subtropical gyre. Environ. Microbiol. **11**: 2291–2300. doi:10.1111/j.1462-2920.2009.01954.x

Flerus, R., O. J. Lechtenfeld, B. P. Koch, S. L. McCallister, P. Schmitt-Kopplin, R. Benner, K. Kaiser, and G. Kattner. 2012. A molecular perspective on the ageing of marine dissolved organic matter. Biogeosciences **9**: 1935–1955. doi: 10.5194/bg-9-1935-2012

Fletcher, M. 1996. Bacterial adhesion: Molecular and ecological diversity. Wiley.

Gifford, S. M., S. Sharma, M. Booth, and M. A. Moran. 2013. Expression patterns reveal niche diversification in a marine microbial assemblage. ISME J. **7**: 281–298. doi:10.1038/ismej.2012.96

Giovannoni, S. J. 2017. SAR11 bacteria: The most abundant plankton in the oceans. Ann. Rev. Mar. Sci. **9**: 12.1–12.25. doi: 10.1146/annurev-marine-010814-015934

Giovannoni, S. J., M. S. Rappe, K. L. Vergin, and N. L. Adair. 1996. 16S rRNA genes reveal stratified open ocean bacterioplankton populations related to the green non-sulfur bacteria. Proc. Natl. Acad. Sci. U. S. A. **93**: 7979–7984. doi:10.1073/pnas.93.15.7979

Giovannoni, S. J., and others. 2005. Genome streamlining in a cosmopolitan oceanic bacterium. Science **309**: 1242–1245. doi:10.1126/science.1114057

Goldberg, S. J., C. A. Carlson, D. A. Hansell, N. B. Nelson, and D. A. Siegel. 2009. Temporal dynamics of dissolved combined neutral sugars and the quality of dissolved organic matter in the Northwestern Sargasso Sea. Deep-Sea Res. Pt. I. **56**: 672–685.

Goldberg, S. J., C. E. Nelson, D. A. Viviani, C. N. Shulse, and M. J. Church. 2017. Cascading influence of inorganic nitrogen sources on DOM production, composition, lability and microbial community structure in the open ocean. Environ. Microbiol. **19**: 3450–3464. doi:10.1111/1462-2920.13825

Gonzalez, J. M., M. C. Portillo, P. Belda-Ferre, and A. Mira. 2012. Amplification by PCR artificially reduces the proportion of the rare biosphere in microbial communities. PLoS ONE **7**: e29973. doi:10.1371/journal.pone.0029973

Gundersen, K., M. Heldal, S. Norland, D. A. Purdie, and A. H. Knap. 2002. Elemental C, N, and P cell content of individual bacteria collected at the Bermuda Atlantic time-series study (BATS) site. Limnol. Oceanogr. **47**: 1525–1530. doi: 10.4319/lo.2002.47.5.1525

Hallam, S. J., T. J. Mincer, C. Schleper, C. M. Preston, K. Roberts, P. M. Richardson, and E. F. DeLong. 2006. Pathways of carbon assimilation and ammonia oxidation suggested by environmental genomic analyses of marine crenarchaeota. PLoS Biol. **4**: e95. doi:10.1371/journal.pbio.0040095

Hamdan, L. J., J. L. Salerno, A. Reed, S. B. Joye, and M. Damour. 2018. The impact of the deepwater horizon blowout on historic shipwreck-associated sediment microbiomes in the northern Gulf of Mexico. Sci. Rep. **8**: 9057.

Hansell, D. A. 2013. Recalcitrant dissolved organic carbon fractions. Ann. Rev. Mar. Sci. **5**: 421–445. doi:10.1146/annurev-marine-120710-100757

Hansell, D. A., and C. A. Carlson. 2001. Biogeochemistry of total organic carbon and nitrogen in the Sargasso Sea: Control by convective overturn. Deep-Sea Res. Pt. II. **48**: 1649–1667.

Hansell, D. A., C. A. Carlson, and R. Schlitzer. 2012. Net removal of major marine dissolved organic carbon fractions in the subsurface ocean. Global Biogeochem. Cycles **26**: GB1016. doi:10.1029/2011GB004069

Hedges, J. I., R. G. Keil, and R. Benner. 1997. What happens to terrestrial organic matter in the ocean? Org. Geochem. **27**: 195–212. doi:10.1016/S0146-6380(97)00066-1

Henrichs, S. M. 1991. Methods of sample handling and analysis for dissolved and particulate amino acids and carbohydrates in seawater. Geoph. Monog. Series **63**: 139–149. doi: 10.1029/GM063p0139

Herndl, G. J., T. Reinthaler, E. Teira, H. van Aken, C. Veth, A. Pernthaler, and J. Pernthaler. 2005. Contribution of

Archaea to total prokaryotic production in the deep Atlantic Ocean. Appl. Environ. Microb. **71**: 2303–2309. doi:10.1128/AEM.71.5.2303-2309.2005

Hertkorn, N., R. Benner, M. Frommberger, P. Schmitt-Kopplin, M. Witt, K. Kaiser, A. Kettrup, and J. I. Hedges. 2006. Characterization of a major refractory component of marine dissolved organic matter. Geochim. Cosmochim. Acta **70**: 2990–3010. doi:10.1016/j.gca.2006.03.021

Hoffmann, K., C. Hassenruck, V. Salman-Carvalho, M. Holtappels, and C. Bienhold. 2017. Response of bacterial communities to different detritus compositions in Arctic deep-sea sediments. Front. Microbiol. **8**: 266. doi:10.3389/fmicb.2017.00266

Holert, J., E. Cardenas, L. H. Bergstrand, E. Zaikova, A. S. Hahn, S. J. Hallam, and W. W. Mohn. 2018. Metagenomes reveal global distribution of bacterial steroid catabolism in natural, engineered, and host environments. MBio **9**: e02345–17. doi:10.1128/mBio.02345-17

Hu, P., and others. 2017. Simulation of Deepwater horizon oil plume reveals substrate specialization within a complex community of hydrocarbon degraders. Proc. Natl. Acad. Sci. U. S. A. **114**: 7432–7437. doi:10.1073/pnas.1703424114

Hwang, C. Y., and B. C. Cho. 2009. Spongiibacter tropicus sp nov., isolated from a Synechococcus culture. Int. J. Syst. Evol. Micr. **59**: 2176–2179. doi:10.1099/ijs.0.005819-0

Iverson, V., R. M. Morris, C. D. Frazar, C. T. Berthiaume, R. L. Morales, and E. V. Armbrust. 2012. Untangling genomes from metagenomes: Revealing an uncultured class of marine Euryarchaeota. Science **335**: 587–590. doi:10.1126/science.1212665

Jean, W. D., Y. T. Yeh, S. P. Huang, J. S. Chen, and W. Y. Shieh. 2016. Spongiibacter taiwanensis sp nov., a marine bacterium isolated from aged seawater. Int. J. Syst. Evol. Micr. **66**: 4094–4098. doi:10.1099/ijsem.0.001316

Johnson, W. M., M. C. Kido Soule, and E. B. Kujawinski. 2017. Extraction efficiency and quantification of dissolved metabolites in targeted marine metabolomics. Limnol. Oceanogr. Methods **15**: 417–428. doi:10.1002/lom3.10181

Kaiser, K., and R. Benner. 2009. Biochemical composition and size distribution of organic matter at the Pacific and Atlantic time-series stations. Mar. Chem. **113**: 63–77. doi:10.1016/j.marchem.2008.12.004

Kalscheuer, R., and others. 2007. Analysis of storage lipid accumulation in Alcanivorax borkumensis: Evidence for alternative triacylglycerol biosynthesis routes in bacteria. J. Bacteriol. **189**: 918–928. doi:10.1128/JB.01292-06

Kamalanathan, M., and others. 2018. Extracellular enzyme activity profile in a chemically enhanced water accommodated fraction of surrogate oil: Toward understanding microbial activities after the deepwater horizon oil spill. Front. Microbiol. **9**: 798. doi:10.3389/fmicb.2018.00798

Karner, M. B., E. F. DeLong, and D. M. Karl. 2001. Archaeal dominance in the mesopelagic zone of the Pacific Ocean. Nature **409**: 507–510. doi:10.1038/35054051

Kawasaki, N., and R. Benner. 2006. Bacterial release of dissolved organic matter during cell growth and decline: Molecular origin and composition. Limnol. Oceanogr. **51**: 2170–2180. doi:10.4319/lo.2006.51.5.2170

Keil, R. G., and D. L. Kirchman. 1999. Utilization of dissolved protein and amino acids in the northern Sargasso Sea. Aquat. Microb. Ecol. **18**: 293–300. doi:10.3354/ame018293

Kellerman, A. M., F. Guillemette, D. C. Podgorski, G. R. Aiken, K. D. Butler, and R. G. M. Spencer. 2018. Unifying concepts linking dissolved organic matter composition to persistence in aquatic ecosystems. Environ. Sci. Technol. **52**: 2538–2548. doi:10.1021/acs.est.7b05513

Kido Soule, M. C., K. Longnecker, W. M. Johnson, and E. B. Kujawinski. 2015. Environmental metabolomics: Analytical strategies. Mar. Chem. **177**: 374–387. doi:10.1016/j.marchem.2015.06.029

Kim, S. H., Y. K. Shin, Y. C. Sohn, and H. C. Kwon. 2012. Two new cholic acid derivatives from the marine ascidian-associated bacterium Hasllibacter halocynthiae. Molecules **17**: 12357–12364. doi:10.3390/molecules171012357

Klappenbach, J. A., J. M. Dunbar, and T. M. Schmidt. 2000. rRNA operon copy number reflects ecological strategies of bacteria. Appl. Environ. Microbiol. **66**: 1328–1333. doi:10.1128/AEM.66.4.1328-1333.2000

Koch, B. P., and T. Dittmar. 2016. From mass to structure: An aromaticity index for high-resolution mass data of natural organic matter. Rapid Commun. Mass Spectrom. **30**: 250–250. doi:10.1002/rcm.7433

Koch, B. P., G. Kattner, M. Witt, and U. Passow. 2014. Molecular insights into the microbial formation of marine dissolved organic matter: Recalcitrant or labile? Biogeosciences **11**: 4173–4190. doi:10.5194/bg-11-4173-2014

Konneke, M., A. E. Bernhard, J. R. de la Torre, C. B. Walker, J. B. Waterbury, and D. A. Stahl. 2005. Isolation of an autotrophic ammonia-oxidizing marine archaeon. Nature **437**: 543–546. doi:10.1038/nature03911

Kramer, G. D., and G. J. Herndl. 2004. Photo- and bioreactivity of chromophoric dissolved organic matter produced by marine bacterioplankton. Aquat. Microb. Ecol. **36**: 239–246. doi:10.3354/ame036239

Kuznetsova, M., and C. Lee. 2002. Dissolved free and combined amino acids in nearshore seawater, sea surface microlayers and foams: Influence of extracellular hydrolysis. Aquat. Sci. **64**: 252–268. doi:10.1007/s00027-002-8070-0

Landry, Z., B. K. Swan, G. J. Herndl, R. Stepanauskas, and S. J. Giovannoni. 2017. SAR202 genomes from the dark ocean predict pathways for the oxidation of recalcitrant dissolved organic matter. MBio **8**: e00413–17. doi:10.1128/mBio.00413-17

Lauro, F. M., and others. 2009. The genomic basis of trophic strategy in marine bacteria. Proc. Natl. Acad. Sci. U. S. A. **106**: 15527–15533. doi:10.1073/pnas.0903507106

Lazar, C. S., B. J. Baker, K. W. Seitz, and A. P. Teske. 2017. Genomic reconstruction of multiple lineages of uncultured benthic archaea suggests distinct biogeochemical roles and ecological niches. ISME J. **11**: 1118–1129. doi:10.1038/ismej.2016.189

Lechtenfeld, O. J., G. Kattner, R. Flerus, S. L. McCallister, P. Schmitt-Kopplin, and B. P. Koch. 2014. Molecular transformation and degradation of refractory dissolved organic matter in the Atlantic and Southern Ocean. Geochim. Cosmochim. Acta **126**: 321–337. doi:10.1016/j.gca.2013.11.009

Lee, C., and C. Cronin. 1982. The vertical flux of particulate organic nitrogen in the sea - decomposition of amino-acids in the Peru upwelling area and the equatorial Atlantic. J. Mar. Res. **40**: 227–251.

Lee, S. H., and J. A. Fuhrman. 1991. Species composition shift of confined bacterioplankton studied at the level of community DNA. Mar. Ecol. Prog. Ser. **79**: 195–201. doi:10.3354/meps079195

Lee, K., H. K. Lee, T. H. Choi, and J. C. Cho. 2007. Robiginitomaculum antarcticum gen. nov., sp. nov., a member of the family Hyphomonadaceae, from Antarctic seawater. Int. J. Syst. Evol. Microbiol. **57**: 2595–2599. doi:10.1099/ijs.0.65274-0

Lekunberri, I., E. Sintes, D. de Corte, T. Yokokawa, and G. J. Herndl. 2013. Spatial patterns of bacterial and archaeal communities along the Romanche fracture zone (tropical Atlantic). FEMS Microbiol. Ecol. **85**: 537–552. doi:10.1111/1574-6941.12142

Lengger, S. K., J. Fromont, and K. Grice. 2017. Tapping the archives: The sterol composition of marine sponge species, as determined non-invasively from museum-preserved specimens, reveals biogeographical features. Geobiology **15**: 184–194. doi:10.1111/gbi.12206

Li, H., P. B. Shinde, H. J. Lee, E. S. Yoo, C. O. Lee, J. Hong, S. H. Choi, and J. H. Jung. 2009. Bile acid derivatives from a sponge-associated bacterium Psychrobacter sp. Arch. Pharm. Res. **32**: 857–862. doi:10.1007/s12272-009-1607-1

Lindroth, P., and K. Mopper. 1979. High-performance liquid-chromatographic determination of subpicomole amounts of amino-acids by precolumn fluorescence derivatization with ortho-phthaldialdehyde. Anal. Chem. **51**: 1667–1674. doi:10.1021/ac50047a019

Liu, Z., S. Liu, J. Liu, and W. S. Gardner. 2013. Differences in peptide decomposition rates and pathways in hypoxic and oxic coastal environments. Mar. Chem. **157**: 67–77. doi:10.1016/j.marchem.2013.08.003

Liu, J. Q., H. P. Bacosa, and Z. F. Liu. 2017. Potential environmental factors affecting oil-degrading bacterial populations in deep and surface waters of the northern Gulf of Mexico. Front. Microbiol. **7**: 2131. doi:10.3389/fmicb.2016.02131

Lonborg, C., X. A. Alvarez-Salgado, K. Davidson, and A. E. J. Miller. 2009. Production of bioavailable and refractory dissolved organic matter by coastal heterotrophic microbial populations. Estuar. Coast. Shelf Sci. **82**: 682–688. doi:10.1016/j.ecss.2009.02.026

Longnecker, K. 2015. Dissolved organic matter in newly formed sea ice and surface seawater. Geochim. Cosmochim. Acta **171**: 39–49. doi:10.1016/j.gca.2015.08.014

Lu, X., S. Sun, J. T. Hollibaugh, and X. Mou. 2015. Identification of polyamine-responsive bacterioplankton taxa in South Atlantic bight. Environ. Microbiol. Rep. **7**: 831–838. doi:10.1111/1758-2229.12311

Lu, K. J., W. S. Gardner, and Z. F. Liu. 2018. Molecular structure characterization of riverine and coastal dissolved organic matter with ion mobility quadrupole time-of-flight LCMS (IM Q-TOF LCMS). Environ. Sci. Technol. **52**: 7182–7191. doi:10.1021/acs.est.8b00999

Mann, P. J., and others. 2014. Evidence for key enzymatic controls on metabolism of Arctic river organic matter. Glob. Chang. Biol. **20**: 1089–1100. doi:10.1111/gcb.12416

Martínez-Pérez, A. M., H. Osterholz, M. Nieto-Cid, M. Alvarez, T. Dittmar, and X. A. Alvarez-Salgado. 2017. Molecular composition of dissolved organic matter in the Mediterranean Sea. Limnol. Oceanogr. **62**: 2699–2712. doi:10.1002/lno.10600

Math, R. K., H. M. Jin, J. M. Kim, Y. Hahn, W. Park, E. L. Madsen, and C. O. Jeon. 2012. Comparative genomics reveals adaptation by Alteromonas sp. SN2 to marine tidal-flat conditions: Cold tolerance and aromatic hydrocarbon metabolism. PLoS ONE **7**: e35784. doi:10.1371/journal.pone.0035784

McCarren, J., J. W. Becker, D. J. Repeta, Y. Shi, C. R. Young, R. R. Malmstrom, S. W. Chisholm, and E. F. DeLong. 2010. Microbial community transcriptomes reveal microbes and metabolic pathways associated with dissolved organic matter turnover in the sea. Proc. Natl. Acad. Sci. U. S. A. **107**: 16420–16427.

McMurdie, P. J., and S. Holmes. 2013. Phyloseq: An R package for reproducible interactive analysis and graphics of microbiome census data. PLoS ONE **8**: e61217. doi:10.1371/journal.pone.0061217

Medeiros, P. M., M. Seidel, L. C. Powers, T. Dittmar, D. A. Hansell, and W. L. Miller. 2015. Dissolved organic matter composition and photochemical transformations in the northern North Pacific Ocean. Geophys. Res. Lett. **42**: 863–870. doi:10.1002/2014GL062663

Mehrshad, M., F. Rodriguez-Valera, M. A. Amoozegar, P. Lopez-Garcia, and R. Ghai. 2018. The enigmatic SAR202 cluster up close: Shedding light on a globally distributed dark ocean lineage involved in sulfur cycling. ISME J. **12**: 655–668. doi:10.1038/s41396-017-0009-5

Morris, R. M., M. S. Rappe, S. A. Connon, K. L. Vergin, W. A. Siebold, C. A. Carlson, and S. J. Giovannoni. 2002. SAR11 clade dominates ocean surface bacterioplankton communities. Nature **420**: 806–810. doi:10.1038/nature01240

Morris, R. M., M. S. Rappe, E. Urbach, S. A. Connon, and S. J. Giovannoni. 2004. Prevalence of the Chloroflexi-related

SAR202 bacterioplankton cluster throughout the mesopelagic zone and deep ocean. Appl. Environ. Microb. **70**: 2836–2842. doi:10.1128/AEM.70.5.2836-2842.2004

Morris, R. M., K. L. Vergin, J. C. Cho, M. S. Rappe, C. A. Carlson, and S. J. Giovannoni. 2005. Temporal and spatial response of bacterioplankton lineages to annual convective overturn at the Bermuda Atlantic time-series study site. Limnol. Oceanogr. **50**: 1687–1696. doi:10.4319/lo.2005.50.5.1687

Muller, O., L. Seuthe, G. Bratbak, and M. L. Paulsen. 2018. Bacterial response to permafrost derived organic matter input in an Arctic fjord. Front. Mar. Sci. **5**: 263. doi:10.3389/fmars.2018.00263

Neufeld, J. D., H. Schäfer, M. J. Cox, R. Boden, I. R. McDonald, and J. C. Murrell. 2007. Stable-isotope probing implicates *Methylophaga* spp and novel *Gammaproteobacteria* in marine methanol and methylamine metabolism. ISME J. **1**: 480–491. doi:10.1038/ismej.2007.65

Noell, S. E., and S. J. Giovannoni. 2019. SAR11 bacteria have a high affinity and multifunctional glycine betaine transporter. Environ. Microbiol. **21**: 2559–2575. doi:10.1111/1462-2920.14649

Oksanen, J., R. Kindt, P. Legendre, B. O'Hara, M H. H Stevens, M. Oksanen, and M. Suggests. 2007. The vegan package. Community ecology package. **10**: 631–637.

Orsi, W. D., and others. 2016. Diverse, uncultivated bacteria and archaea underlying the cycling of dissolved protein in the ocean. ISME J. **10**: 2158–2173. doi:10.1038/ismej.2016.20

Osterholz, H., J. Niggemann, H. A. Giebel, M. Simon, and T. Dittmar. 2015. Inefficient microbial production of refractory dissolved organic matter in the ocean. Nat. Commun. **6**: 7422. doi:10.1038/ncomms8422

Parsons, R. J., M. Breitbart, M. W. Lomas, and C. A. Carlson. 2012. Ocean time-series reveals recurring seasonal patterns of virioplankton dynamics in the northwestern Sargasso Sea. ISME J. **6**: 273–284. doi:10.1038/ismej.2011.101

Parsons, R. J., and others. 2015. Marine bacterioplankton community turnover within seasonally hypoxic waters of a subtropical sound: Devil's hole, Bermuda. Environ. Microbiol. **17**: 3481–3499. doi:10.1111/1462-2920.12445

Patriarca, C., J. Bergquist, P. J. R. Sjoberg, L. Tranvik, and J. A. Hawkes. 2018. Online HPLC-ESI-HRMS method for the analysis and comparison of different dissolved organic matter samples. Environ. Sci. Technol. **52**: 2091–2099. doi:10.1021/acs.est.7b04508

Pedler, B. E., L. I. Aluwihare, and F. Azam. 2014. Single bacterial strain capable of significant contribution to carbon cycling in the surface ocean. Proc. Natl. Acad. Sci. U. S. A. **111**: 7202–7207. doi:10.1073/pnas.1401887111

Pérez, M. T., C. Pausz, and G. J. Herndl. 2003. Major shift in bacterioplankton utilization of enantiomeric amino acids between surface waters and the ocean's interior. Limnol. Oceanogr. **48**: 755–763. doi:10.4319/lo.2003.48.2.0755

Perminova, I. V., F. H. Frimmel, A. V. Kudryavtsev, N. A. Kulikova, G. Abbt-Braun, S. Hesse, and V. S. Petrosyan. 2003. Molecular weight characteristics of humic substances from different environments as determined by size exclusion chromatography and their statistical evaluation. Environ. Sci. Technol. **37**: 2477–2485. doi:10.1021/es0258069

Polz, M. F., D. E. Hunt, S. P. Preheim, and D. M. Weinreich. 2006. Patterns and mechanisms of genetic and phenotypic differentiation in marine microbes. Philos. Trans. R. Soc. Lond. B Biol. Sci. **361**: 2009–2021. doi:10.1098/rstb.2006.1928

Porter, K. G., and Y. S. Feig. 1980. The use of DAPI for identifying and counting aquatic microflora. Limnol. Oceanogr. **25**: 943–948. doi:10.4319/lo.1980.25.5.0943

Rappe, M. S., S. A. Connon, K. L. Vergin, and S. J. Giovannoni. 2002. Cultivation of the ubiquitous SAR11 marine bacterioplankton clade. Nature **418**: 630–633. doi:10.1038/nature00917

Ravenschlag, K., K. Sahm, and R. Amann. 2001. Quantitative molecular analysis of the microbial community in marine arctic sediments (Svalbard). Appl. Environ. Microbiol. **67**: 387–395. doi:10.1128/AEM.67.1.387-395.2001

Redmond, M. C., and D. L. Valentine. 2012. Natural gas and temperature structured a microbial community response to the Deepwater horizon oil spill. Proc. Natl. Acad. Sci. U. S. A. **109**: 20292–20297. doi:10.1073/pnas.1108756108

Repeta, D. J. 2015. Chemical characterization and cycling of dissolved organic matter, p. 21–63. *In* D. A. Hansell and C. A. Carlson [eds.], Biogeochemistry of marine dissolved organic matter. Academic.

Ridlon, J. M., and P. B. Hylemon. 2012. Identification and characterization of two bile acid coenzyme a transferases from Clostridium scindens, a bile acid 7 alpha-dehydroxylating intestinal bacterium. J. Lipid Res. **53**: 66–76. doi:10.1194/jlr.M020313

Romera-Castillo, C., H. Sarmento, X. A. Alvarez-Salgado, J. M. Gasol, and C. Marrase. 2011. Net production and consumption of fluorescent colored dissolved organic matter by natural bacterial assemblages growing on marine phytoplankton exudates. Appl. Environ. Microb. **77**: 7490–7498. doi:10.1128/AEM.00200-11

Saw, J. H. W., and others. In Press. Pangenomics reveal diversification of enzyme families and niche specialization in globally abundant SAR202 bacteria. MBio. doi:10.1128/mBio.02975-19

Schattenhofer, M., B. M. Fuchs, R. Amann, M. V. Zubkov, G. A. Tarran, and J. Pernthaler. 2009. Latitudinal distribution of prokaryotic picoplankton populations in the Atlantic Ocean. Environ. Microbiol. **11**: 2078–2093. doi:10.1111/j.1462-2920.2009.01929.x

Schmidt, F., and others. 2017. Unraveling signatures of biogeochemical processes and the depositional setting in the molecular composition of pore water DOM across different marine environments. Geochim. Cosmochim. Acta **207**: 57–80. doi:10.1016/j.gca.2017.03.005

Schneiker, S., and others. 2006. Genome sequence of the ubiquitous hydrocarbon-degrading marine bacterium Alcanivorax borkumensis. Nature Biotechnol. **24**: 997–1004. doi:10.1038/nbt1232

Sherwood, B. P., E. A. Shaffer, K. Reyes, K. Longnecker, L. I. Aluwihare, and F. Azam. 2015. Metabolic characterization of a model heterotrophic bacterium capable of significant chemical alteration of marine dissolved organic matter. Mar. Chem. **177**: 357–365. doi:10.1016/j.marchem.2015.06.027

Sieracki, M. E., C. L. Viles, and K. L. Webb. 1989. Algorithm to estimate cell biovolume using image analyzed microscopy. Cytometry **10**: 551–557. doi:10.1002/cyto.990100510

Sleighter, R. L., and P. G. Hatcher. 2009. Molecular characterization of dissolved organic matter (DOM) along a river to ocean transect of the lower Chesapeake Bay by ultrahigh resolution electrospray ionization Fourier transform ion cyclotron resonance mass spectrometry. Mar. Chem. **110**: 140–152. doi:10.1016/j.marchem.2008.04.008

Sperling, M., H. A. Giebel, B. Rink, S. Grayek, J. Staneva, E. Stanev, and M. Simon. 2012. Differential effects of hydrographic and biogeo chemical properties on the SAR11 clade and Roseobacter RCA cluster in the North Sea. Aquat. Microb. Ecol. **67**: 25–34. doi:10.3354/ame01580

Spring, S., and T. Riedel. 2013. Mixotrophic growth of bacteriochlorophyll a-containing members of the OM60/NOR5 clade of marine gammaproteobacteria is carbon-starvation independent and correlates with the type of carbon source and oxygen availability. BMC Microbiol. **13**: 117. doi:10.1186/1471-2180-13-117

Spring, S., C. Scheuner, M. Goker, and H. P. Klenk. 2015. A taxonomic framework for emerging groups of ecologically important marine gammaproteobacteria based on the reconstruction of evolutionary relationships using genome-scale data. Front. Microbiol. **6**: 281. doi:10.3389/fmicb.2015.00281

Sprouffske, K. 2018. Package 'growthcurver'. https://github.com/sprouffske/growthcurver, DOI: 10.1371/journal.pgen.1007324.

Stewart, F. J., T. Dalsgaard, C. R. Young, B. Thamdrup, N. P. Revsbech, O. Ulloa, D. E. Canfield, and E. F. DeLong. 2012. Experimental incubations elicit profound changes in community transcription in OMZ bacterioplankton. PLoS ONE **7**: e37118. doi:10.1371/journal.pone.0037118

Stoica, E., and G. J. Herndl. 2007. Contribution of Crenarchaeota and Euryarchaeota to the prokaryotic plankton in the coastal northwestern Black Sea. J. Plankton Res. **29**: 699–706. doi:10.1093/plankt/fbm051

Suttle, C. A., A. M. Chan, and J. A. Fuhrman. 1991. Dissolved free amino-acids in the Sargasso Sea - uptake and respiration rates, turnover times, and concentrations. Mar. Ecol. Prog. Ser. **70**: 189–199. doi:10.3354/meps070189

Teira, E., T. Reinthaler, A. Pernthaler, J. Pernthaler, and G. J. Herndl. 2004. Combining catalyzed reporter deposition-fluorescence in situ hybridization and microautoradiography to detect substrate utilization by bacteria and archaea in the deep ocean. Appl. Environ. Microb. **70**: 4411–4414. doi:10.1128/AEM.70.7.4411-4414.2004

Teira, E., H. van Aken, C. Veth, and G. J. Herndl. 2006. Archaeal uptake of enantiomeric amino acids in the mesopelagic and bathypelagic waters of the North Atlantic. Limnol. Oceanogr. **51**: 60–69. doi:10.4319/lo.2006.51.1.0060

Terrisse, F., C. Cravo-Laureau, C. Noel, C. Cagnon, A. J. Dumbrell, T. J. McGenity, and R. Duran. 2017. Variation of oxygenation conditions on a hydrocarbonoclastic microbial community reveals Alcanivorax and Cycloclasticus ecotypes. Front. Microbiol. **8**: 1549. doi:10.3389/fmicb.2017.01549

Thrash, J. C., K. W. Seitz, B. J. Baker, B. Temperton, L. E. Gillies, N. N. Rabalais, B. Henrissat, and O. U. Mason. 2017. Metabolic roles of uncultivated bacterioplankton lineages in the northern Gulf of Mexico "dead zone". MBio **8**: e01017–17. doi:10.1128/mBio.01017-17

Tolbert, A., H. Akinosho, R. Khunsupat, A. K. Naskar, and A. J. Ragauskas. 2014. Characterization and analysis of the molecular weight of lignin for biorefining studies. Biofuels Bioprod. Biorefin. **8**: 836–856. doi:10.1002/bbb.1500

Tourna, M., and others. 2011. Nitrososphaera viennensis, an ammonia oxidizing archaeon from soil. Proc. Natl. Acad. Sci. U. S. A. **108**: 8420–8425. doi:10.1073/pnas.1013488108

Treusch, A. H., S. Leininger, A. Kletzin, S. C. Schuster, H. P. Klenk, and C. Schleper. 2005. Novel genes for nitrite reductase and Amo-related proteins indicate a role of uncultivated mesophilic crenarchaeota in nitrogen cycling. Environ. Microbiol. **7**: 1985–1995. doi:10.1111/j.1462-2920.2005.00906.x

Treusch, A. H., K. L. Vergin, L. A. Finlay, M. G. Donatz, R. M. Burton, C. A. Carlson, and S. J. Giovannoni. 2009. Seasonality and vertical structure of microbial communities in an ocean gyre. ISME J. **3**: 1148–1163. doi:10.1038/ismej.2009.60

Varela, M. M., H. M. van Aken, and G. J. Herndl. 2008. Abundance and activity of Chloroflexi-type SAR202 bacterioplankton in the meso- and bathypelagic waters of the (sub)tropical Atlantic. Environ. Microbiol. **10**: 1903–1911. doi:10.1111/j.1462-2920.2008.01627.x

Vergin, K. L., and others. 2013. High-resolution SAR11 ecotype dynamics at the Bermuda Atlantic time-series study site by phylogenetic placement of pyrosequences. ISME J. **7**: 1322–1332. doi:10.1038/ismej.2013.32

Vorobev, A., and others. 2018. Identifying labile DOM components in a coastal ocean through depleted bacterial transcripts and chemical signals. Environ. Microbiol. **20**: 3012–3030. doi:10.1111/1462-2920.14344

Walker, C. B., and others. 2010. *Nitrosopumilus maritimus* genome reveals unique mechanisms for nitrification and autotrophy in globally distributed marine crenarchaea. Proc. Natl. Acad. Sci. U. S. A. **107**: 8818–8823. doi:10.1073/pnas.0913533107

Wang, K., L. Zou, X. Lu, and X. Mou. 2018. Organic carbon source and salinity shape sediment bacterial composition in two China marginal seas and their major tributaries. Sci. Total Environ. **633**: 1510–1517. doi:10.1016/j.scitotenv.2018.03.295

Wear, E. K., C. A. Carlson, A. K. James, M. A. Brzezinski, L. A. Windecker, and C. E. Nelson. 2015. Synchronous shifts in dissolved organic carbon bioavailability and bacterial community responses over the course of an upwelling-driven phytoplankton bloom. Limnol. Oceanogr. **60**: 657–677. doi:10.1002/lno.10042

Webster, N. S., and T. Thomas. 2016. The sponge hologenome. MBio **7**: e00135–e00116. doi:10.1128/mBio.00135-16

Weiss, M. S., U. Abele, J. Weckesser, W. Welte, E. Schiltz, and G. E. Schulz. 1991. Molecular architecture and electrostatic properties of a bacterial porin. Science **254**: 1627–1630. doi:10.1126/science.1721242

Whelan, J. K. 1977. Amino-acids in a surface sediment core of Atlantic abyssal plain. Geochim. Cosmochim. Acta **41**: 803–810. doi:10.1016/0016-7037(77)90050-3

Wilhelm, R. C., R. Singh, L. D. Eltis, and W. W. Mohn. 2018. Bacterial contributions to delignification and lignocellulose degradation in forest soils with metagenomic and quantitative stable isotope probing. ISME J. **13**: 413–429. doi:10.1038/s41396-018-0279-6

Xie, W., and others. 2018. Localized high abundance of Marine Group II archaea in the subtropical Pearl River estuary: Implications for their niche adaptation. Environ. Microbiol. **20**: 734–754. doi:10.1111/1462-2920.14004

Xue, J. H., C. Lee, S. G. Wakeham, and R. A. Armstrong. 2011. Using principal components analysis (PCA) with cluster analysis to study the organic geochemistry of sinking particles in the ocean. Org. Geochem. **42**: 356–367. doi:10.1016/j.orggeochem.2011.01.012

Yakimov, M. M., P. N. Golyshin, S. Lang, E. R. Moore, W. R. Abraham, H. Lunsdorf, and K. N. Timmis. 1998. Alcanivorax borkumensis gen. nov., sp. nov., a new, hydrocarbon-degrading and surfactant-producing marine bacterium. Int. J. Syst. Bacteriol. **48**: 339–348. doi:10.1099/00207713-48-2-339

Yooseph, S., and others. 2010. Genomic and functional adaptation in surface ocean planktonic prokaryotes. Nature **468**: 60–66. doi:10.1038/nature09530

Zark, M., J. Christoffers, and T. Dittmar. 2017. Molecular properties of deep-sea dissolved organic matter are predictable by the central limit theorem: Evidence from tandem FT-ICR-MS. Mar. Chem. **191**: 9–15. doi:10.1016/j.marchem.2017.02.005

Zhang, Y., E. Sintes, M. N. Chen, Y. Zhang, M. H. Dai, N. Z. Jiao, and G. J. Herndl. 2009. Role of mesoscale cyclonic eddies in the distribution and activity of Archaea and Bacteria in the South China Sea. Aquat. Microb. Ecol. **56**: 65–79. doi:10.3354/ame01324

Zhang, C. L. L., W. Xie, A. B. Martin-Cuadrado, and F. Rodriguez-Valera. 2015. Marine group II Archaea, potentially important players in the global ocean carbon cycle. Front. Microbiol. **6**: 1108. doi:10.3389/fmicb.2015.01108

Acknowledgments

We thank Z. Landry for the inspiring idea of SAR202 catabolism of CRAM. We thank the University of California, Santa Barbara Marine Science Institute Analytical Laboratory for analyzing inorganic nutrient samples. We thank C. Johnson for her help in FISH sample processing and BATS group in supporting our project. We thank N. K. Rubin-Saika and R. Padula for their help with amino acid sample preparation. We thank Z. Liu, J. Xue, K. Lu, and Y. Shen for their help with amino acid protocol development and validation. We thank B. Stephens for his help on microscopic image analysis. We thank M. Dasenko and the staff of the CGRB at Oregon State University for amplicon library preparation and DNA sequencing. We are grateful for the help provided by the officers and crews of the R/V *Atlantic Explorer*. Bermuda Institute of Ocean Sciences (BIOS) provides us tremendous support in terms of facilities and lab space. We thank Bermuda government for its allowance of our water sampling and sample export (export permit number SP160904, issued 07 October 2016 under the Fisheries Act, 1972). This project was supported by Simons Foundation International's BIOS-SCOPE program.

Conflict of Interest

None declared

Submitted 29 March 2019
Revised 06 September 2019
Accepted 27 November 2019

Associate editor: Bo Thamdrup